

Rigorous Error Analysis for Logarithmic Number Systems

THANH SON NGUYEN, Kahlert School of Computing - The University of Utah, USA

ALEXEY SOLOVYEV, Kahlert School of Computing - The University of Utah, USA

GANESH GOPALAKRISHNAN, Kahlert School of Computing - The University of Utah, USA

Logarithmic Number Systems (LNS) hold considerable promise in helping reduce the number of bits needed to represent a high dynamic range of real-numbers with finite precision, and also efficiently support multiplication and division. However, under LNS, addition and subtraction turn into non-linear functions that must be approximated—typically using precomputed table-based functions. Additionally, multiple layers of error correction are typically needed to improve result accuracy. Unfortunately, previous efforts have not characterized the resulting error bound. We provide the first rigorous analysis of LNS, covering detailed techniques such as *co-transformation* that are crucial to implement subtraction with reasonable accuracy. We provide theorems capturing the error due to table interpolations, the finite precision of pre-computed values in the tables, and the error introduced by fix-point multiplications involved in LNS implementations. We empirically validate our analysis using a Python implementation, showing that our analytical bounds are tight, and that our testing campaign generates inputs diverse-enough to almost match (but not exceed) the analytical bounds. We close with discussions on how to adapt our analysis to LNS systems with different bases and also discuss many pragmatic ramifications of our work in the broader arena of scientific computing and machine learning.

CCS Concepts: • **Mathematics of computing** → **Solvers**; *Mathematical software performance*.

Additional Key Words and Phrases: Number Systems, Floating-Point Arithmetic, Fixed-Point numbers, Error Analysis

CONTENTS

Abstract	1
Contents	1
1 Introduction	2
2 Related Work	5
3 Background, Notations	6
4 High Level Overview of Entire Error Analysis	12
4.1 Error analysis for First-Order Taylor Approximation	12
4.2 Error analysis for the Error Correction technique	13
4.3 Error analysis for the Co-transformation technique	16
5 Rigorous error bound of first-Order Taylor approximation	17
6 Rigorous error bound of the error correction technique	19
7 Rigorous error bound of the co-transformation technique	24
8 Numerical experiments	26
8.1 Numerical verification of error-bound	26
8.2 Magnitude of error-bound over parameters	34
9 Concluding Remarks	38
9.1 Contribution	38
9.2 Future Directions	38

Authors' addresses: Thanh Son Nguyen, Kahlert School of Computing - The University of Utah, Utah, USA; Alexey Solovyev, Kahlert School of Computing - The University of Utah, Utah, USA; Ganesh Gopalakrishnan, Kahlert School of Computing - The University of Utah, Utah, USA.

References	39
A Proof of the correctness of the co-transformation technique	40
B Proof of Lemma 5.2	41
C Proof of Lemma 6.6	41

1 INTRODUCTION

With the increasing costs of data movement in today’s HPC and ML applications [1, 2], there is significant pressure to reduce the number of bits used to represent real numbers using finite-precision representations. With fewer bits moved, memory bandwidth as well as cache memories are better utilized. Also, given the sheer number of scalar multiplications carried out by these applications (e.g., when performing matrix and tensor products), those number representations that help reduce multiplication (and division) costs are also of great importance. Logarithmic number systems (LNS) possess both these advantages. They store only the logarithm of real numbers in *finite-precision fixed-point representations*¹. Furthermore, multiplications and divisions turn into fixed-point addition and fixed-point subtraction (respectively); and in the absence of overflows, are exact. Also, square-root turns into division by 2 (right shift), thus exact.

Addition and subtraction are a whole different story, turning into calculations involving non-linear functions. This requires good trade-offs between error control and computational speed. In more detail, methods are needed to perform additions and subtractions with techniques to perform *multiple levels of error correction* using various lookup tables whose overall cost must be minimized.²

However, despite the availability of these error correction methods, *there are no rigorous error analysis methods available that tightly bound the worst-case error*. This is quite an odd situation: on one hand, we have methods to compensate for errors. On the other hand, no one has produced a tight bound on the worst-case error. Our work in this paper closes this gap by providing such a rigorous error bound.

All existing error estimation techniques that we know of perform error estimations through empirical testing. It is well-known that without tight error bounds, actual hardware/software designs most likely will end up over-provisioning to accomodate for these “excess errors” that never occur. The key contribution of this paper is the first such tight and rigorous bound parameterized over today’s popular LNS schemes. Specifically,

- We provide the first tight parametric error estimate formulae in terms of parameters such as the machine-epsilon of fixed-point numbers as well as look-up table sizes. Such a parameterization can help precisely guide hardware and software implementations.
- We demonstrate through systematic testing using a Python implementation of LNS that our hand-derived estimates are trustworthy *and tight*. We release this code to enable others to reproduce and further validate our work.

A more rigorous mechanical verification is not attempted at this stage for the following reasons:

- None of the existing SMT-based [3–5] automated tools are sufficiently powerful to check the validity our derivations.

¹In virtually all LNS implementations that are surveyed later.

²“Tableless methods” are also popular, approximating what table-based methods provide, but are not studied in this work.

- Our analytical results and the manner in which we decompose their proofs are similar to those necessary in any attempt at mechanical proofs using expert-guided proof-checkers—efforts that are typically multi-year, and beyond the scope of this paper.

Comparison of LNS and IEEE Floating-Point. For those familiar with IEEE floating-point arithmetic [6], an IEEE *normal* floating-point number is described by a triple (s, e, m) , where $s \in \{-1, 1\}$ denotes the sign, $e \in \mathbb{Z}$ is the exponent and $m \in [1, 2)$ is the mantissa (also known as the significant). The value of the real number represented by this triple is $s \cdot (2^e) \cdot m$. Unlike floating-point, LNS does not have the mantissa but allows rational exponent instead. Also, while a *subnormal* IEEE floating-point number has $m < 1$ (in which case its value is encoded by the value in the mantissa weighted by the smallest normal exponent), LNS does not have the notion of subnormals: the entire representable number scale is modeled in the same manner. Specifically, an LNS number is described by a pair (s, e) , where $s \in \{-1, 1\}$ denotes the sign and $e \in \mathbb{Q}$ is the exponent. This pair represents the real value $s \cdot 2^e$. The exponent part of LNS is represented by a signed fixed-point number with a special arrangement to represent 0.

Rounding modes for LNS. Analogous to IEEE floating-point, two consecutive LNS fixed-point words define an interval of real-numbered values, and any real-number falling in this interval may be rounded up, down, or to the nearest value. The upper-bound of this distance of rounding (depending on the rounding mode) defines the *machine-epsilon* of LNS, which we denote by ϵ in the rest of this paper.

Rigorous Problem Statement. We now introduce some basic notions underlying LNS that allow us to define the problem a bit more tightly. First, we describe how the four basic operations: addition, subtraction, multiplication and division are performed in LNS (operations such as square-root are not described, for brevity). In all four operations, the sign and magnitude of the result can be computed separately. Because computing the sign is straightforward, to make it easy to read, we assume that all the operands are positive to demonstrate how LNS computes the magnitude of the result. Let $2^p, 2^q$ be real numbers which can be exactly represented in LNS by the two fixed-point numbers p, q , then multiplication and division of 2^p and 2^q can be performed efficiently and exactly in LNS by fixed-point addition and subtraction:

$$\begin{aligned}\log_2(2^p \times 2^q) &= \log_2 2^{p+q} = p + q \\ \log_2(2^p / 2^q) &= \log_2 2^{p-q} = p - q\end{aligned}$$

However, the main drawback is that addition and subtraction are not directly realizable in LNS. Without loss of generality, let $p \geq q$ and let us use $x \leq 0$ to denote $q - p$ (this allows us to write 2^x , knowing that it will be a fraction in $(0, 1]$). Then,

$$\begin{aligned}\log_2(2^p + 2^q) &= \log_2(2^p(1 + 2^x)) = i + \log_2(1 + 2^x) \\ \log_2(2^p - 2^q) &= \log_2(2^p(1 - 2^x)) = i + \log_2(1 - 2^x)\end{aligned}$$

Now let us introduce two non-linear functions Φ^+ and Φ^- (plotted in Figure 1, and also called *Gaussian Logarithm* [7]) defined as:

$$\Phi^+(x) = \log_2(1 + 2^x) \quad \text{and} \quad \Phi^-(x) = \log_2(1 - 2^x)$$

In Section 3, we will show that Φ^+ and Φ^- will be approximated via ROM tables look-up and interpolation. Thus, to compute $\log_2(2^p + 2^q)$, we can simply perform a *fixed-point addition of p* to the result of $\Phi^+(x)$ (likewise for $\log_2(2^p - 2^q)$).

In this paper, we focus on deriving the bounds for the absolute-errors of the approximations of Φ^+ and Φ^- , for convenience, we call them *error-bounds* by default.

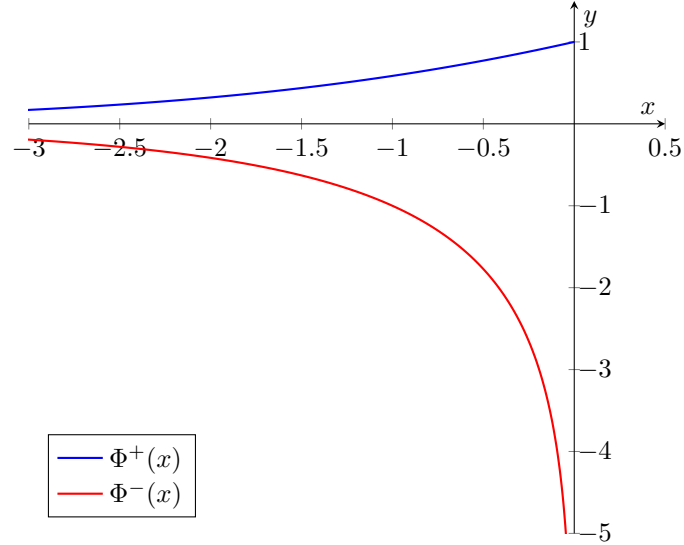


Fig. 1. Plots of $\Phi^+(x)$ and $\Phi^-(x)$

Rigorous error-bound derivation. We derived the error-bound of the three most popular Φ^+/Φ^- approximation techniques which are proposed in European Logarithm Microprocessor [8]. These techniques will be described in detail in Section 3. To derive the rigorous error-bounds, firstly, we analyze all error sources of each technique, which include the errors of the mathematical nature of the approximation method and the errors of finite-precision hardware implementation. Then, we mathematically derive the error-bound of each error source by symbolic function analysis, and finally accumulate them using the absolute-norm inequality. The mathematics derivations are performed manually with significant support from the Sympy [9] library, which handles symbolic expression manipulations. Details of all error sources considered in our analysis are mentioned in Section 4 and details of error-bounds derivations for each source are presented in Sections 5, 6 and 7.

Validation of Rigorous Analysis: Key Results. In our validation of our bound tightness, we compute the values of Φ^+ and Φ^- over large and dense input sample sets, and across different LNS configurations. We then compare the results against the results of direct computation of our analytical formulae—all using extended precision. From our experimental results, the fact that none of the errors exceeds the error-bounds computed using our error-bound formulae. We also control our test-case generation process to produce instances where the error is very close to (but never exceeds) the error-bounds. We provide detailed histograms of inputs showing that the concentration of inputs where these inputs are low, but non-zero—all this going to support the correctness and tightness of our derived error-bound formulae.

Organization. In Section 2, we survey existing LNS approaches that we are aware of. Section 3 introduces some background and the notations used in our derivations. Because of the tedious and detailed nature of our error analysis, in Section 4, we will present all of our derivations via plots and intuitive explanations. Then, Section 5 contains the details of error-bound derivation of first-order Taylor approximation (can be skipped upon first reading). Also, Section 6 and Section 7 contain the details of error-bound derivation of the error-correction technique and the co-transformation technique (also can be skipped upon first reading). Section 8 checks our analysis through numerical experiments.

Section 9 describes adaptations of the LNS we analyze to other LNS—showing the possibility of easily carrying over our approach to these other LNS without deriving their error-bounds from scratch, then our conclusions and future work.

Code Release: We publish our github repository at <https://github.com/Thanhson89/RigorousErrorLNS>, which includes the tool for calculating LNS’s rigorous error-bound with respect to the user’s input parameters and the result of our experiments in Section 8, and details of symbolic algebra tools used.

2 RELATED WORK

Proposed in the early 1970s, LNS are still a topic of current active interest. Many of these proposed schemes have been realized in software. An LNS-based implementation of weight updates in neural network training was recently proposed by NVIDIA [10] where a hardware implementation is proposed. A recent hardware implementation of the Ising model [11] also employs the LNS. A bibliography of over 600 citations relevant to LNS research has been provided by XLNS Research [12].

Unfortunately, *no prior work has derived rigorous error bounds*, which is our main contribution here. We now briefly survey prior LNS, citing the logarithm-base used in them, how addition and subtraction are realized, whether a hardware implementation exists, and the status of error analysis to the extent we are aware of.

European Logarithm Microprocessor [13]. This is a historically important piece of work resulting in the first complete hardware realization of an LNS microprocessor. This LNS scheme uses base-2 logarithm. It employs the error-correction algorithms for the approximation of $\Phi^\pm(x) = \log(1 \pm 2^x)$, and also employs the co-transformation technique [14] for Φ^- when $x \rightarrow 0$ (both these ideas are detailed in Section 3). These authors evaluate the area and delay of their LNS implementation, showing that while the area for the LNS realization is equivalent to that of floating-point implementations, the delay could be much better. Although the authors compare the error of LNS with that of floating-point through empirical testing, there is no rigorous error analysis for LNS.

Low-precision LNS beyond Base-2 [15]. In this LNS scheme, the logarithm base is in the range $\sqrt{2}$ to 2. The base is selected so as to optimize the approximation error of the inputs as well as the sizes of addition/subtraction truth tables. This paper also suggests that it is more efficient to implement these tables using logic gates rather than using ROM. Hardware implementations are proposed, and error analysis is achieved via simulation for conversion and single-operators.

Semi-LNS [16]. This number system is a hybrid between Floating-point and LNS, which consists of both of rational logarithmic and mantissa parts, for balancing the efficiency between multiplication/division and addition/subtraction. Although there is some error analysis for representation error, that of operations’ error is not mentioned.

ROM-less LNS. This LNS design is tailored for minimal hardware implementation. The computation of addition and subtraction is based on Mitchell’s method [17], which is very efficient to be implemented on hardware with the trade-off of accuracy. Some approaches have been proposed to improve the accuracy of Mitchell’s method, such as using operand decomposition [18], base selection [19], and Approximate tableless LNS ALU [20].

Convolution Neural Networks (CNN) Using Logarithmic Data Representations [21]. In this approach, the logarithm base is 2 as well as $\sqrt{2}$. This approach proposes the first CNN implemented in low-precision LNS and showing that LNS is superior to fixed-point arithmetic in such implementation because of the non-uniform distribution of weights and

activations. This scheme has not been implemented in hardware as far as we know, neither has rigorous analysis has been conducted.

LogNet [22]. In this approach, the logarithm bases used are 2 and $\sqrt{2}$. This work focuses on improving the learning algorithm of CNNs using LNS, demonstrating the superiority of LNS over fixed-point schemes in terms of hardware costs. While there is a hardware implementation, rigorous error analysis has not been attempted.

LNS-MADAM [10]. In this scheme, the logarithm base used is $2^{1/k}$. The highlight of their work is proposing a training algorithm for Deep Neural Networks (DNN) in low-precision LNS with an approximation of addition technique and the Multiplicative Weight Update (MWU) algorithm to replace Stochastic Gradient Descent. The authors propose their own LNS’s design and hardware implementation, which is based on Mitchell’s method and stochastic rounding [23]. The paper also performs symbolic error analysis just for the sake of indicating that Multiplicative Weight Update is superior to Stochastic Gradient Descent in terms of minimizing the quantization error-bound. However, the error-bound is not approximated tightly enough to provide insight to the accuracy of their LNS’s design and implementation.

Comparison: Our rigorous analysis is applicable to all these LNS variants, as it is parametric over the base of the logarithm, and accommodates various precision choices and table-based implementations.

3 BACKGROUND, NOTATIONS

Let us consider LNS implementations where multiplication and division (which turn into addition and subtraction, respectively) are suitably guarded against overflows (for example, by checking that the underlying fixed-point addition and subtraction do not overflow or underflow). The rest of this paper concentrates on addition and subtraction.

The computation of LNS addition and subtraction involves addition/subtraction and interpolations with respect to tables that discretize the Φ^+ and Φ^- functions, suitably limiting the number of pre-computed and stored table values. Let Φ generically stand for either Φ^+ or Φ^- .

When it is necessary to make it clear that we are indexing tables, we will use the notation Φ_T . We will sample Φ at a spacing of Δ and store these values in Φ_T . Now, given an arbitrary x , define i as $\left\lceil \frac{x}{\Delta} \right\rceil \Delta$ and r as $i - x$. We have $x = i - r$ ³. Recall that x is negative. Thus, i is the discrete index *after* x . It must be clear that $\Phi_T(i) = \Phi(i)$ and $\Phi_T(x)$ (viewed as a tabular function) is undefined at other x than at these i . For x not in Φ_T , we can apply interpolation techniques [8, 13, 24] that we will explain in detail, to make this paper self-contained.

Approximating $\Phi(x)$ through Taylor Approximation, yielding function $\hat{\Phi}_T$. We can now define an approximation to $\Phi(x)$ defined with the help of the two tables Φ_T and Φ'_T that are defined at the i points:

$$\hat{\Phi}_T(x) = \Phi(i) - r\Phi'(i) = \Phi_T(i) - r\Phi'_T(i) \quad (1)$$

Example 1: First-order Taylor approximation

This example illustrates how $\Phi^+(x)$ is calculated using first-order Taylor approximation. All the numerical values in this example are in binary. Let the signed fixed-point representation of the LNS consist of 1 integer bit and 8 fractional bits. The two look-up tables $\Phi_T^+(x)$ and $(\Phi_T^+)'(x)$ are shown in Table 1 ($\Delta = 0.10000000$).

³Strictly we must use i_x and r_x as they depend on x ; but we prefer i and r for readability.

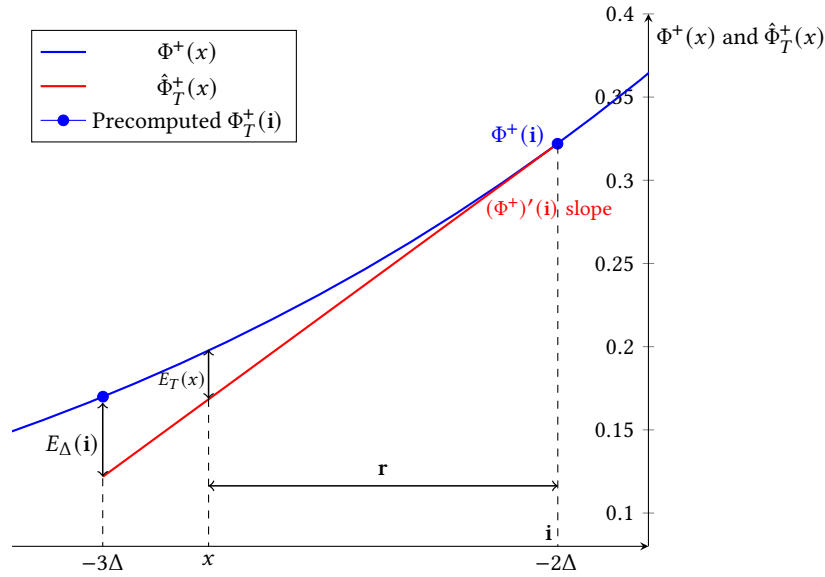


Fig. 2. Details of defining $E_{\Delta}(i)$

i	$\Phi_T^+(i)$	i	$(\Phi_T^+)'(i)$
-0.00000000	1.00000000	-0.00000000	0.10000000
-0.10000000	0.11000110	-0.10000000	0.01101010
-1.00000000	0.10010110	-1.00000000	0.01010101
-1.10000000	0.01110000	-1.10000000	0.01000011

Table 1. Illustration of LNS via an example: two look-up tables Φ_T^+ and $(\Phi_T^+)'$ for performing First-order Taylor approximation (see Equation 1) are created

Suppose that we want to calculate $\Phi^+(x)$ with $x = -0.11000000$:

- (1) First, determine the index value i above x , which turns out to be $i = -0.10000000$. This is r above x , where $r = i - x = 0.01000000$.
- (2) Next, look up $\Phi^+(i)$ and $(\Phi^+)'(i)$, obtaining $\Phi^+(-0.10000000) = 0.10010110$ and $(\Phi^+)'(-0.10000000) = 0.01101010$.
- (3) Finally, $\Phi^+(x)$ using First-order Taylor approximation (Equation 1) is

$$\begin{aligned} \hat{\Phi}_T^+(x) &= \Phi_T^+(i) - r(\Phi_T^+)'(i) \\ &= 0.10010110 - 0.01000000 \times 0.01101010 = 0.01111011 \end{aligned}$$

For higher accuracy, the European Logarithmic Microprocessor [8, 13] suggests adding an **error-correction** term to the previous formula because a linear interpolation is too coarse. Let us refer to the difference between the mathematical $\Phi(x)$ and the just now defined approximation $\hat{\Phi}_T(x)$ by a new “error function” $E_T(x)$, which is plotted in Figure 3. A key observation made in [8, 13] is that if all the “spikes” of $E_T(x)$ bounded by Δ - are scaled such that the tips of the

spikes are 1, such a scaled function, now called $P(x)$, becomes nearly periodic, as shown in Figure 4. This “error-ratio function” can be defined as follows:

$$P(x) = E_T(x)/E_\Delta(i) \quad (2)$$

where $E_\Delta(i)$ is the supremum of E_T in the Δ -segment $(i - \Delta, i]$ containing x . In other words, $E_\Delta(i) = \lim_{x \rightarrow (i-\Delta)} E_T(x)$. Figure 2 shows that this can be written as $\Phi(i - \Delta) - \Phi(i) + \Delta\Phi'(i)$ or even as $\Phi_T(i - \Delta) - \Phi_T(i) + \Delta\Phi'_T(i)$

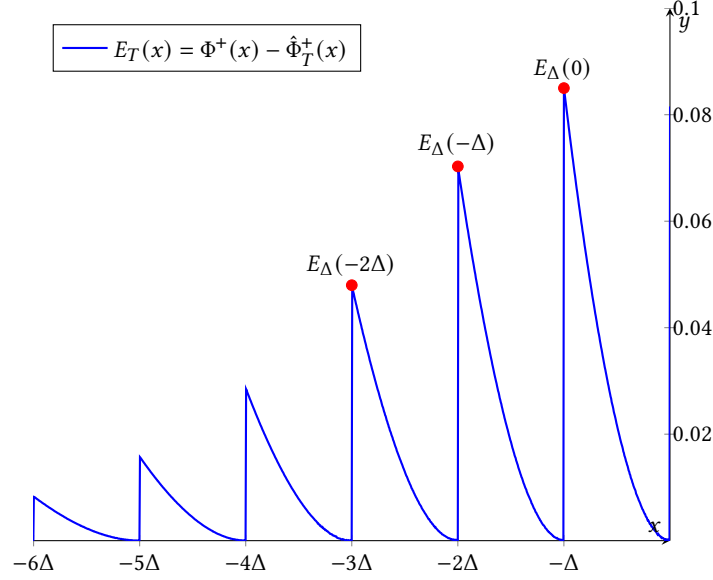
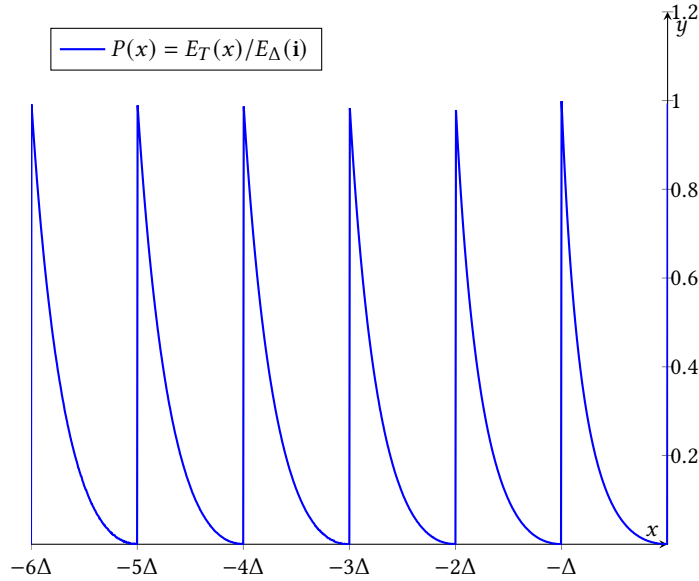


Fig. 3. We do first-order Taylor approximation of $\Phi(x)$, obtaining $\hat{\Phi}_T$. This still has an error E_T . We plot E_T^+ here.

While function $P(x)$ looks periodic, strictly it is not; i.e., it does not satisfy $P(x) = P(x - \Delta)$ but *it nearly does*. We can exploit this fact by choosing an arbitrary repeating segment of $P(x)$ and normalizing our calculations with respect to that segment. More formally,

- Let $k \in \mathbb{N}$ and let $c = k\Delta$.
- Then precompute the values of $P(x)$ inside this c -th segment, filling a new table called P_c (this table depends on the choice of c).
- When we index P_c at $r \in [0, \Delta)$ (we will later make it clear what the resolution of r is), we are obtaining $P(c - r)$, and this corresponds to the ratio $E_T(c - r)/E_\Delta(c)$.
- Now we can approximate $P(x)$ using the P_c table by using $P(x) \approx P(c + i - x) = P_c(r)$.
- Next, we create another lookup table E_Δ that delivers the E_T values at all i using the “original” first-order Taylor approximations. More specifically, $E_\Delta(i) = \Phi(i - \Delta) - \Phi(i) + \Delta\Phi'(i)$.
- The size and index values of this E_Δ table are the same as those of the look-up tables for Φ_T and Φ'_T .

With all this, $E_T(x)$ can be approximated by the **error-correction term** $E_\Delta(i)P_c(r)$, which is *added* to the first-order Taylor interpolation formula to derive a more accurate approximation (we add this correction because, as is clear from Figure 2, the original $\hat{\Phi}_T(x)$ function consistently delivers values smaller than the true $\Phi(x)$ function):

Fig. 4. Error ratio $P(x)$ in each Δ interval

$$\hat{\Phi}_{EC}(x) = \hat{\Phi}_T(x) + E_\Delta(\mathbf{i})P_c(\mathbf{r}) = \Phi_T(\mathbf{i}) - \mathbf{r}\Phi'_T(\mathbf{i}) + E_\Delta(\mathbf{i})P_c(\mathbf{r}) \quad (3)$$

where $E_\Delta(\mathbf{i}) = \Phi_T(\mathbf{i} - \Delta) - \Phi_T(\mathbf{i}) + \Delta\Phi'_T(\mathbf{i})$ and $P_c(\mathbf{r}) = E_T(c - \mathbf{r})/E_\Delta(c)$.

We refer to this definition of $\Phi_{EC}(x)$ as **computing using the error correction technique**, requiring altogether four look-up tables: one for E_Δ indexed by \mathbf{i} , one for P_c indexed by \mathbf{r} , and the former two tables Φ_T and Φ'_T .

Example 2: Error-correction technique

This example illustrates how $\Phi^+(x)$ is calculated using the error-correction technique. The fixed-point representation of the LNS and two look-up tables of Φ^+ and $(\Phi^+)'$ are exactly the same as those of Example 1. The two look-up tables for E_Δ and P_c are shown in Table 2.

\mathbf{i}	$E_\Delta(\mathbf{i})$	\mathbf{r}	$P_c(\mathbf{r})$
-0.00000000	0.00000110	0.00000000	0.00000000
-0.10000000	0.00000101	0.00100000	0.00001111
-1.00000000	0.00000101	0.01000000	0.01000001
-1.10000000	0.00000100	0.01100000	0.10101010

Table 2. Illustration of LNS via an example: two look-up tables of E_Δ and P_c for performing error-correction technique (see Equation 3)

We want to calculate $\Phi^+(x)$ for the same value of $x = -0.11000000$ as in Example 1:

- (1) Firstly, we calculate $\Phi^+(x)$ by First-order Taylor approximation and get $\hat{\Phi}_T^+(x) = 0.10000000$ (see Example 1). The values of $\mathbf{i} = -0.10000000$ and $\mathbf{r} = 0.01000000$ are also the same as those in Example 1.

- (2) Secondly, we look up the values of $E_{\Delta}(\mathbf{i})$ and $P_c(\mathbf{r})$ in the two look-up tables and get: $E_{\Delta}(-0.10000000) = 0.00000101$ and $P_c(0.01000000) = 0.01000001$. Note that in case \mathbf{r} is not in the table P_c , we take the values from the closest index. Then, we calculate the error-correction term:

$$E_{\Delta}(\mathbf{i})P_c(\mathbf{r}) = 0.00000101 \times 0.01000001 = 0.00000001$$

- (3) Finally, we add the error-correction term to the First-ordered Taylor approximation (see Equation 3) and get:

$$\hat{\Phi}_{EC}^+(x) = \hat{\Phi}_T^+(x) + E_{\Delta}(\mathbf{i})P_c(\mathbf{r}) = 0.01111011 + 0.00000001 = 0.01111100$$

Co-transformation: Error control when x approaches 0: One of the more difficult cases of error control in LNS is when computing $\Phi^-(x)$ for values of x is close to 0. The trouble arises because of the nature of this function: the n th derivative of $\Phi^-(x)$ for all n tend to $-\infty$ as x approaches 0, i.e. $\Phi^-(x)$ has a singularity at 0 (see Figure 1). To avoid computing $\Phi^-(x)$ in this range, addition/subtraction can be split across different intervals and computed by the so-called *co-transformation* techniques [14, 25–28]. The state-of-the-art co-transformation technique is proposed by European Logarithmic Microprocessor [14, 29], which suggests 3-way interval split defined by design-specific constants Δ_a and Δ_b . The general idea is to maintain three extra look-up tables T_a, T_b and T_c of Φ^- inside the range $(-1, 0)$, then transform $\Phi^-(x)$ such that it can be computed by indexing those look-up tables together with interpolating Φ^- outside of the range $(-1, 0)$. Specifically, the three look-up tables T_a, T_b and T_c , then the co-transformation technique are described as follows (see Appendix A for the proof of correctness):

Let Δ_a and Δ_b are two positive fixed-point numbers such that Δ_a is very close to 0, Δ_b is a multiple of Δ_a and a divisor of 1:

- The table T_a covers all fixed-point numbers in a very small range $[-\Delta_a, 0)$,
- The table T_b covers all multiples of Δ_a in the range $[-\Delta_b, -\Delta_a)$.
- The table T_c covers all multiples of Δ_b in the range $x \in (-1, -\Delta_b)$.

When x in $(-1, 0)$, the value of x must belong to one of the three cases: $x \in [-\Delta_a, 0)$, $x \in [-\Delta_b, -\Delta_a)$ and $x \in (-1, -\Delta_b)$.:

The formulae for $\Phi^-(x)$ is derived across the three cases as follows:

- **Case 1:** $x \in [-\Delta_a, 0)$: $\Phi^-(x)$ is indexed directly from table T_a .

- **Case 2:** $x \in [-\Delta_b, -\Delta_a)$:

Let $r_b = \left(\left\lceil \frac{x}{\Delta_a} \right\rceil - 1\right)\Delta_a$, (i.e. r_b is the index value of T_b which is smaller than and closest to x)

and $r_a = r_b - x$,

and let $k = x - \Phi^-(r_b) + \Phi^-(r_a)$.

Then

$$\Phi^-(x) = \Phi^-(r_b) + \Phi^-(k) \tag{4}$$

where $\Phi^-(r_a)$ and $\Phi^-(r_b)$ are indexed directly from tables T_a and T_b respectively, and $\Phi^-(k)$ is computed by interpolation (either by first-order Taylor approximation or the error-correction technique).

- **Case 3:** $x \in (-1, -\Delta_b)$:

Let $r_c = \left(\left\lceil \frac{x}{\Delta_b} \right\rceil - 1\right)\Delta_b$, (i.e. r_c is the index value of T_c which is smaller than and closest to x)

and $r_{ab} = r_c - x$,

and $r_b = \left(\left\lfloor \frac{r_{ab}}{\Delta_a} \right\rfloor - 1 \right) \Delta_a$, (i.e. r_b is the index value of T_b which is smaller than and closest to r_{ab})
 and $r_a = r_b - r_{ab}$,
 and $k_1 = r_{ab} + \Phi^-(r_a) - \Phi^-(r_b)$,
 and $k_2 = x + \Phi^-(r_b) + \Phi^-(k_1) - \Phi^-(r_c)$.

Then

$$\Phi^-(x) = \Phi^-(r_c) + \Phi^-(k_2) \quad (5)$$

where $\Phi^-(r_a)$, $\Phi^-(r_b)$, and $\Phi^-(r_c)$ are indexed directly from tables T_a , T_b , and T_c respectively, and $\Phi^-(k_1)$ and $\Phi^-(k_2)$ are computed by interpolation (either by first-order Taylor approximation or error-correction technique). Figure 5 illustrates the positions and meanings of r_c , r_{ab} , r_b and r_a with respect to x .

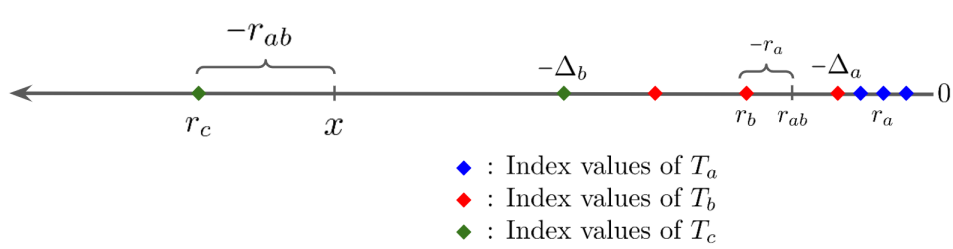


Fig. 5. Co-transformation Illustration for the case where $x \in (-1, -\Delta_b)$: The positions of r_c, r_{ab}, r_b and r_a that are derived from this x are shown. Here, r_c is the closest index value of T_c on the left of x . The gap of x and r_c is $-r_{ab}$. now r_b is the closest index value of T_b on the left of r_{ab} . Finally, the gap of r_{ab} and r_b is $-r_a$.

Example 3: Co-transformation technique

The following example illustrates the computation of $\Phi^-(x)$ using the co-transformation technique. Let the signed fixed-point representation of the LNS consist of 3 integer bits and 6 fractional bits. The co-transformation technique is applied when $x \in (-1, 0)$; otherwise, we use first-order Taylor approximation. Assume that, the two look-up tables of Φ^+ and $(\Phi^+)'$ are pre-computed with $\Delta = 0.01$. Let $\Delta_a = 0.0001$, $\Delta_b = 0.01$, and the three tables T_a, T_b, T_c are shown in Table 3.

T_a	
x	$\Phi^-(x)$
-0.000001	-110.100010
-0.000010	-101.100010
-0.000011	-100.111110

T_b	
x	$\Phi^-(x)$
-0.000100	-100.100100
-0.001000	-11.100110
-0.001100	-11.000010

T_c	
x	$\Phi^-(x)$
-0.010000	-10.101010
-0.100000	-1.110001
-0.110000	-1.010011

Table 3. Illustration of co-transformation via an example. LNS design is represented by fixed-point numbers with 6 fractional bits. The three tables T_a, T_b, T_c in binary with $\Delta_a = 0.000001$, $\Delta_b = 0.0001$, $\Delta_c = 0.01$.

Suppose that we want to compute $\Phi^-(x)$ with $x = -0.000101$. Because $x \in [-\Delta_b, -\Delta_a)$, we apply Case 2's formulae for calculation:

- (1) Firstly, we compute r_b and r_a from the value of x and Δ_b , and get: $r_b = -0.001000$ and $r_a = -0.000011$.

- (2) Before computing k , we need to look up the values of $\Phi^-(r_a)$ and $\Phi^-(r_b)$ from Table 3: $\Phi^-(r_a) = -100.111110$ and $\Phi^-(r_b) = -11.100110$. Then, we compute $k = x - \Phi^-(r_b) + \Phi^-(r_a) = -1.011101$.
- (3) Next, we compute $\Phi^-(k)$ using first-order Taylor approximation (with $\Delta = 0.01$): $\hat{\Phi}_T^-(k) = -0.101001$
- (4) Finally, we compute $\Phi^-(x)$ using Equation 4:

$$\Phi^-(x) \approx \Phi^-(r_b) + \hat{\Phi}_T^-(k) = (-11.100110) + (-0.101001) = -100.001111$$

Error Analysis Conventions. In this paper, we focus on deriving the error-bounds of approximating Φ^+ and Φ^- using the first-order Taylor approximation, the error-correction technique and the co-transformation techniques. The error-bounds are parameterized by that machine-epsilon, ϵ , together with the parameters, which involves in the calculation of the three techniques, such as $\Delta, \Delta_p, \Delta_a$ and Δ_b . There are many other designs of LNS, such as non- $2^{\frac{1}{k}}$ based [10, 15], varied Δ [13], ROM-less [17, 30–32]. Covering all those designs is beyond the scope of this paper. However, in Section 9, we will show how the error-bound can be slightly modified for some popular LNS designs.

4 HIGH LEVEL OVERVIEW OF ENTIRE ERROR ANALYSIS

In this section, we consecutively analyze all the sources that cause error of computing Φ^+ and Φ^- by the three techniques mentioned in Section 3: first-order Taylor approximation, error-correction, and co-transformation. Then, we provide an overview of how the derivation of the rigorous error-bound for each technique proceeds, which will be described in detail in Sections 5, 6, 7, giving each error mnemonic names (§4.1)⁴

4.1 Error analysis for First-Order Taylor Approximation

Earlier, in Equation 1, we discussed how to mathematically calculate Φ^+ and Φ^- via first-order Taylor approximation, the error of which was illustrated in Figure 3. However, because LNS is implemented in hardware using fixed-point numbers, there are two more sources of error due to the fact that the look-up tables' values of $\Phi(i)$ and $\Phi'(i)$ must be rounded to the current LNS's fixed-point representation, and the multiplication $\mathbf{r}\Phi'(i)$ is performed in fixed-point arithmetic (with rounding). Taking into account the implementation using fixed-point, we refine the first-order Taylor approximation presented in Equation 1 as:

$$\tilde{\Phi}_T(x) = \bar{\Phi}(i) - \text{rnd}(\mathbf{r}\bar{\Phi}'(i)) \quad (6)$$

where $\bar{\Phi}$ and $\bar{\Phi}'$ are the fixed-point rounded look-up tables for Φ and Φ' .

We define the notations for the three sources of error:

- Interp-err: the mathematical error of interpolating Φ^+ and Φ^- via first-order Taylor approximation, which is $|\Phi(x) - \hat{\Phi}_T(x)|$
- Tab-err: the rounding error of the pre-computed values in the look-up tables, which are $|\Phi(i) - \bar{\Phi}(i)|$ and $|\Phi'(i) - \bar{\Phi}'(i)|$.
- Mul-err: the error of fixed-point arithmetic multiplication, which is $|\mathbf{r}\bar{\Phi}'(i) - \text{rnd}(\mathbf{r}\bar{\Phi}'(i))|$.

The error of interpolating Φ using first-order Taylor approximation is $|\Phi(x) - \tilde{\Phi}_T(x)|$, where $\tilde{\Phi}_T(x)$ is defined in Equation 6. The rigorous error-bound is derived as follows.

⁴We exclude the range $(-1, 0)$ for $\Phi^-(x)$, as this function tends to negative infinity, and hence co-transformation is needed to meaningfully handle this range; this will be detailed in Section 7).

Error-bound of Interp-err derivation: Lemma 5.1 and Lemma 5.2 consecutively derive the error-bound of the Interp-err for Φ^+ and Φ^- , without considering Tab-err and Mul-err. Intuitively, from the shape of Interp-err of Φ^+ (illustrated in Figure 3), we observe that:

- For each Δ -segment, the error is greater when x is further away from 0.
- The further a Δ -segment is away from 0, the smaller its supremum error is.

Lemma 5.1 formally proves those observations by analyzing the error-function $|\Phi^+(x) - \hat{\Phi}_T^+(x)|$ and conclude that the supremum of the error over the whole domain $x < 0$ is approached when $x \rightarrow -\Delta$. Similarly, Lemma 5.2 proves that the error-bound of Φ^- is obtained when $x \rightarrow -1 - \Delta$.

Total error-bound derivation: The error-bound of Tab-err and Mul-err is simply a constant ϵ , which is the maximum absolute rounding error of the LNS' fixed-point representation. The total error-bound is derived in Theorem 5.3 by accumulating (using absolute-norm inequality) the error-bound of Interp-err with that of Tab-err and Mul-err.

4.2 Error analysis for the Error Correction technique

Similar to the previous section, before deriving the error-bound, we refine the mathematical formula of interpolation via error-correction technique (Equation 3) such that it matches with the hardware implementation. In hardware implementation, besides the fact that the look-up tables' values and results of multiplications are rounded according to the LNS' fixed-point representation, we also note that the index values of P_c are evenly spaced with distance Δ_P and any fixed-point number \mathbf{r} is rounded-down to one of these indices $\hat{\mathbf{r}}$ before indexing. Therefore, the formula of interpolation via error-correction technique (Equation 3) is *refined* as:

$$\tilde{\Phi}_{EC}(x) = \overline{\Phi}(\mathbf{i}) + \text{rnd}(\mathbf{r}\overline{\Phi}'(\mathbf{i})) - \text{rnd}(\overline{E}_\Delta(\mathbf{i})\overline{P}_c(\hat{\mathbf{r}})) \quad (7)$$

where $\overline{\Phi}$, $\overline{\Phi}'$, \overline{P}_c , \overline{E}_Δ are the fixed-point rounded look-up tables for Φ , Φ' , P_c and E_Δ .

Next, we analyze the error sources of the refined formula of interpolation via the error-correction technique. The main error of interpolation via the error-correction technique is that of approximating the exact value of the ratio $P(x)$ by the pre-computed term $P_c(\mathbf{r})$ (mentioned earlier in Section 3). Together with the hardware implementation errors above, we define the four sources of error (by splitting Inter-error into two parts shown below):

- Interp-error decomposed into:
 - Ratio-err: the error of approximating $P(x)$ by $P_c(\mathbf{r})$, which is $|P(x) - P_c(\mathbf{r})|$.
 - Index-err: the error caused by rounding \mathbf{r} to an index value $\hat{\mathbf{r}}$ of the table P_c before indexing, which is $|P_c(\mathbf{r}) - P_c(\hat{\mathbf{r}})|$
- Tab-err: the rounding error of the pre-computed values in the look-up tables.
- Mul-err: the rounding error of fixed-point arithmetic multiplication.

The error of interpolating Φ using the error-correction technique is $|\Phi(x) - \tilde{\Phi}_{EC}(x)|$, where $\tilde{\Phi}_{EC}(x)$ is defined in Equation 7. The derivation of the rigorous error-bound of interpolation using error-correction technique is fully described in Section 6. The structure its proof and the roles of the supporting lemmas are shown in Figure 6. The main idea of the proof is summarized as follows.

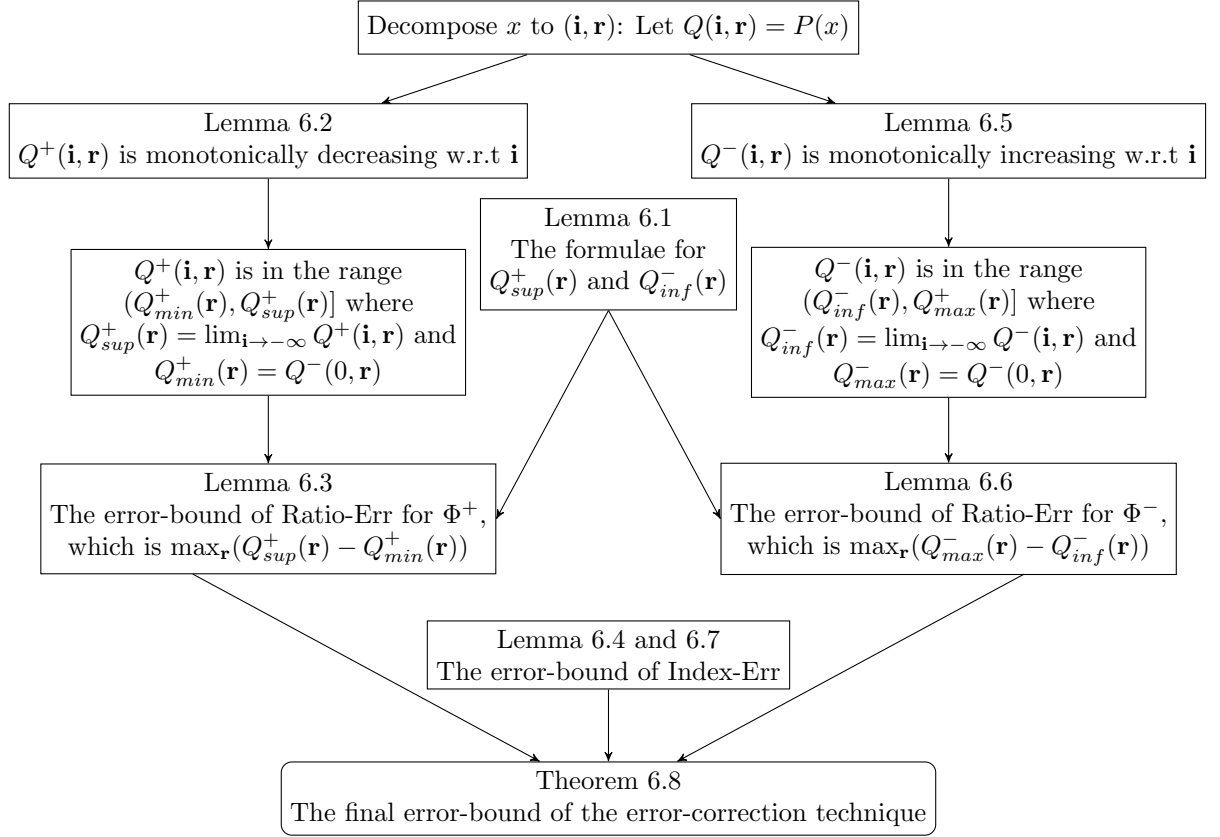


Fig. 6. Derivation diagram of the rigorous error-bound of error correction technique

Error-bound of Ratio-err derivation: We observe that deriving the rigorous error bound for Ratio-err is fairly involved, and proceeds as follows. To facilitate our analysis, we define $Q(\mathbf{i}, \mathbf{r}) = P(x)$ (see Section 3 for the definition of \mathbf{i} and \mathbf{r}). Intuitively, for Φ^+ , we observe that for any value of \mathbf{i} , the value of $Q^+(\mathbf{i}, \mathbf{r})$ is inside a finite range $[Q_{min}^+(\mathbf{r}), Q_{sup}^+(\mathbf{r})]$, where $Q_{sup}^+(\mathbf{r}) = \lim_{\mathbf{i} \rightarrow -\infty} Q^+(\mathbf{i}, \mathbf{r})$ and $Q_{min}^+(\mathbf{r}) = Q^+(0, \mathbf{r})$ (illustrated in Figure 7). This observation is formally proved by Lemma 6.1, which derives the formula of $Q_{sup}^+(\mathbf{r})$, and Lemma 6.2, which proves that $Q^+(\mathbf{i}, \mathbf{r})$ is monotonically decreasing with respect to \mathbf{i} .

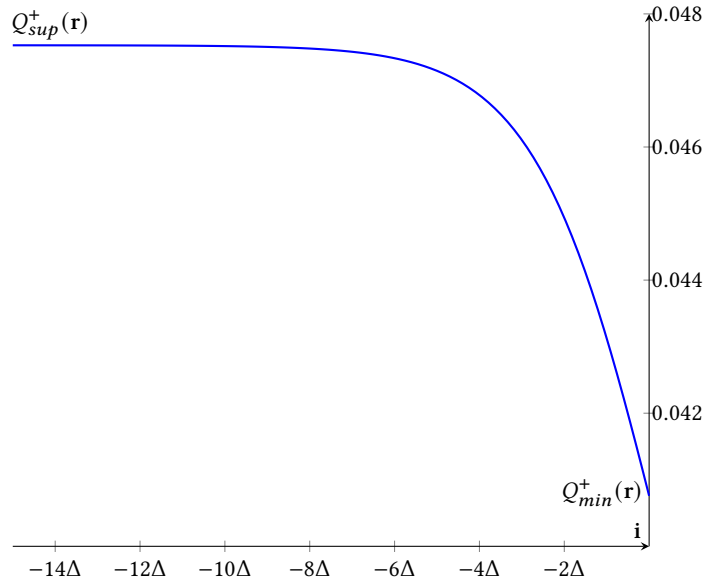


Fig. 7. The range of $Q^+(i, r)$ w.r.t i where $r = 0.2\Delta$

Then, obviously, the error-bound of the Ratio-err is the maximum value of $Q^+_{sup}(r) - Q^+_{min}(r)$ with respect to r . The graph of $Q^+_{sup}(r) - Q^+_{min}(r)$ is illustrated in Figure 8. Lemma 6.3 proves that the function has a single maximum value at r^* in the range $[0, \Delta]$ and derives the formula for r^* . The error-bound of the Ratio-err is obtained by substituting r with r^* in $Q^+_{sup}(r) - Q^+_{min}(r)$.

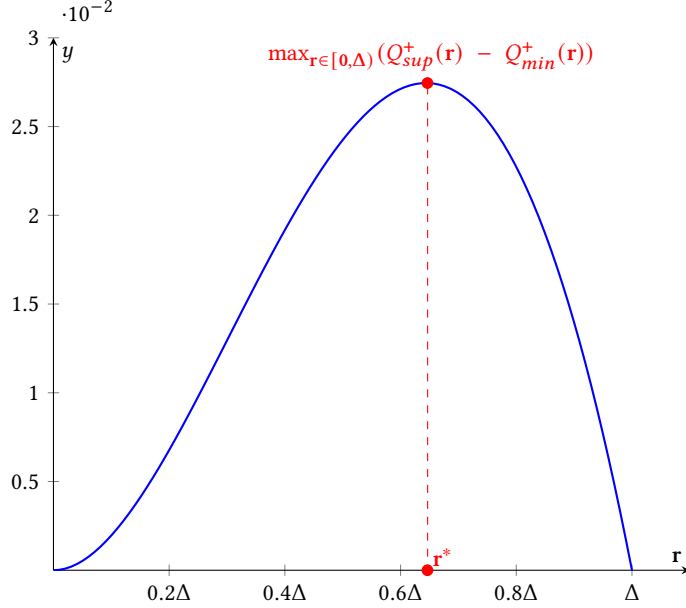


Fig. 8. $Q_{sup}^+(r) - Q_{min}^+(r)$

Error-bound of Index-err derivation: Lemma 6.4 derives the error-bound of Index-err. The key idea of the proof is to show that the supremum of $|Q^+(c, r) - P_c^+(\hat{r})|$ is approached when $r \rightarrow \Delta$ is rounded to $\hat{r} = \Delta - \Delta_P$. This idea comes from the observation that the error-ratio curve (see Figure 4) of each Δ -segment is steepest at the furthest point away from 0 (mathematically, the second derivative of the $Q^+(c, r)$ w.r.t r is negative). Similar steps are done for Φ^- by Lemma 6.5, Lemma 6.6, and Lemma 6.7.

Total error-bound derivation: Finally, Theorem 6.8 derives the formula for the total error-bound of $\tilde{\Phi}_{EC}(x)$, which considers all four sources of errors mentioned above. The total error-bound is derived by accumulating the error-bounds of Ratio-err and Index-err (derived in Lemma 6.3, Lemma 6.4 for Φ^+ and in Lemma 6.6, Lemma 6.7 for Φ^-) with the error-bounds of Tab-err and Mul-err (these two errors are simply the machine-epsilon ϵ).

4.3 Error analysis for the Co-transformation technique

The calculation of all 3 cases of co-transformation technique mentioned at the end of Section 3 involves 5 types of operations/computations: div, subtraction, multiplication (of an integer and a fixed-point number), indexing the value of Φ^- by table look-up, and computing Φ^- by interpolation (using first-order Taylor approximation or error-correction technique). The first 3 operations are error-free in fixed-point arithmetic. Indexing the value of Φ^- by table look-up has the error-bound ϵ . The error-bounds of computing Φ^- by interpolation is derived in subsections 4.1 and 4.2 (details in Section 5 and 6), but with the assumption that the input of the Φ^- function is error-free. However, in the co-transformation technique's calculation, $\Phi^-(k)$ (Case 2), $\Phi^-(k_1)$ (Case 3) and $\Phi^-(k_2)$ (Case 3) are computed by interpolation while the computations of k, k_1 and k_2 contain errors. To address this challenge, we derive the error-bound of $\Phi^-(k)$ from the error-bound of k assuming that the computation of Φ^- is exact (Lemma 7.1), then combine it with the derived error-bound of computing Φ^- by one of the two interpolation techniques. Finally, Theorem 7.2 derives to

total error-bound of computing Φ^- in the range $(-1, 0)$ using the co-transformation technique from the error-bounds of the three cases:

- (1) For Case 1, there is only one look-up table indexing, so the error-bound is simply ϵ
- (2) For Case 2, r_b and r_a are error-free, the error-bound of computing k is 2ϵ (two look-up table indexing of $\Phi^-(r_a)$ and $\Phi^-(r_b)$). Next, the error-bound of computing $\Phi^-(k)$ is derived directly by applying Lemma 7.1. Finally, the total error-bound of computing $\Phi^-(x)$ in Case 2 follows by accumulating one more ϵ , which is the error-bound of indexing $\Phi^-(r_b)$.
- (3) For Case 3, deriving the error-bounds of computing k_1 and $\Phi^-(k_1)$ is similar to that of k and $\Phi^-(k)$ in Case 2. The error-bound of computing k_2 is obtained by accumulating error-bound of computing $\Phi^-(k_1)$ with 2ϵ (two look-up table indexing of $\Phi^-(r_a)$ and $\Phi^-(r_b)$). Similar to Case 2, the error-bound of computing $\Phi^-(k_1)$ is derived by applying Lemma 7.1, and the total error-bound computing $\Phi^-(x)$ in Case 3 follows by accumulating one more ϵ , which is the error-bound of indexing $\Phi^-(r_c)$.

The error-bound of Case 1 is obviously smaller than those of Case 2 and Case 3, so the total error-bound of computing Φ^- in the range $(-1, 0)$ using co-transformation technique is the maximum of the error-bound of Case 2 and Case 3.

5 RIGOROUS ERROR BOUND OF FIRST-ORDER TAYLOR APPROXIMATION

This section mentions in full detail the derivation of the error-bound of calculating Φ^+ and Φ^- using first-order Taylor approximation. The structure of this section and the intuition of the proof were briefly mentioned in Section 4.1:

Lemma 5.1 derive the error-bound of Interp-err of Φ^+ in the range $(-\infty, 0]$. Recall that the Interp-err is $|\Phi^+(x) - \hat{\Phi}^+_T(x)|$ (plotted in Figure 3) and $E_\Delta(\mathbf{i}) = \Phi(\mathbf{i} - \Delta) - \Phi(\mathbf{i}) + \Delta\Phi'(\mathbf{i})$ (defined in Section 3).

LEMMA 5.1. For all $x \in (-\infty, 0]$,

$$|\Phi^+(x) - \hat{\Phi}^+_T(x)| \leq E_\Delta^+(0)$$

PROOF. Let $E(\mathbf{i}, \mathbf{r}) = \Phi^+(x) - \hat{\Phi}^+_T(x)$. From the definition of $\hat{\Phi}^+_T(x)$ in Equation 1:

$$E(\mathbf{i}, \mathbf{r}) = \Phi^+(\mathbf{i} - \mathbf{r}) - (\Phi^+(\mathbf{i}) - \mathbf{r}(\Phi^+)'(\mathbf{i}))$$

Note that despite the definition: $\mathbf{i} = \Delta(x \text{ div } \Delta)$, it is safe to consider the domain of \mathbf{i} to be $\mathbb{R}_{\leq 0}$ instead of $\Delta\mathbb{Z}_{\leq 0}$ when deriving error-bound, because:

$$\max_{\mathbf{i} \in \Delta\mathbb{Z}_{\leq 0}, 0 \leq \mathbf{r} < \Delta} |E(\mathbf{i}, \mathbf{r})| \leq \max_{\mathbf{i} \in \mathbb{R}_{\leq 0}, 0 \leq \mathbf{r} < \Delta} |E(\mathbf{i}, \mathbf{r})| \quad (\text{because } \Delta\mathbb{Z}_{\leq 0} \subset \mathbb{R}_{\leq 0})$$

The lemma is proved by:

- (1) Proving that $\forall \mathbf{i} \leq 0, 0 \leq \mathbf{r} < \Delta : E(\mathbf{i}, \mathbf{r}) \geq 0$, so $E(\mathbf{i}, \mathbf{r}) = |E(\mathbf{i}, \mathbf{r})| = |\Phi^+(x) - \hat{\Phi}^+_T(x)|$
- (2) Proving that both partial derivatives of E w.r.t \mathbf{r} and \mathbf{i} are non-negative, so E approaches its supremum when $\mathbf{i} = 0$ and $\mathbf{r} \rightarrow \Delta$. Formally, we have to prove that $\forall \mathbf{i} \leq 0, 0 \leq \mathbf{r} < \Delta : \frac{\partial E}{\partial \mathbf{r}}(\mathbf{i}, 0) \geq 0$ and $\frac{\partial E}{\partial \mathbf{i}}(\mathbf{i}, 0) \geq 0$, so $\max_{\mathbf{i} \in \mathbb{R}_{\leq 0}, 0 \leq \mathbf{r} < \Delta} E(\mathbf{i}, \mathbf{r}) < E(0, \Delta) = E_\Delta^+(0)$.

First, we take the first and second derivatives of $E(\mathbf{i}, \mathbf{r})$ w.r.t \mathbf{r} :

$$\frac{\partial E}{\partial \mathbf{r}}(\mathbf{i}, \mathbf{r}) = \frac{2^{\mathbf{i}}}{2^{\mathbf{i}+1}} - \frac{2^{\mathbf{i}-\mathbf{r}}}{2^{\mathbf{i}-\mathbf{r}+1}} \quad \text{and} \quad \frac{\partial^2 E}{\partial \mathbf{r}^2}(\mathbf{i}, \mathbf{r}) = \frac{2^{\mathbf{i}-\mathbf{r}} \ln 2}{(2^{\mathbf{i}-\mathbf{r}+1})^2}$$

From $\frac{\partial^2 E}{\partial \mathbf{r}^2}(\mathbf{i}, \mathbf{r}) > 0$ and $\frac{\partial E}{\partial \mathbf{r}}(\mathbf{i}, 0) = 0$, we conclude that $\forall \mathbf{i} \leq 0, 0 \leq \mathbf{r} < \Delta : \frac{\partial E}{\partial \mathbf{r}}(\mathbf{i}, \mathbf{r}) \geq 0$.

Then, because $E(\mathbf{i}, 0) = 0$, we conclude that $\forall \mathbf{i} \leq 0, 0 \leq \mathbf{r} < \Delta : E(\mathbf{i}, \mathbf{r}) \geq 0$.⁵

We complete the proof by proving that $\forall \mathbf{i} \leq 0, 0 \leq \mathbf{r} < \Delta : \frac{\partial E}{\partial \mathbf{i}}(\mathbf{i}, \mathbf{r}) \geq 0$:⁶

If $\mathbf{i} \leq 0, 0 \leq \mathbf{r} < \Delta$, let $a = \mathbf{r} \ln 2$, then

$$\frac{\partial E}{\partial \mathbf{i}}(\mathbf{i}, \mathbf{r}) = \frac{2^{\mathbf{i}}}{(2^{\mathbf{i}} + 1)^2 (2^{1-\mathbf{r}} + 1)} (2^{\mathbf{i}} f(a) + g(a))$$

with $f(a) = ae^{-a} + e^{-a} - 1$ and $g(a) = e^{-a} + a - 1$

Since $\frac{2^{\mathbf{i}}}{(2^{\mathbf{i}} + 1)^2 (2^{1-\mathbf{r}} + 1)} > 0$, the sign of $\frac{\partial E}{\partial \mathbf{i}}(\mathbf{i}, \mathbf{r})$ is the same as that of $N(\mathbf{i}) = 2^{\mathbf{i}} f(a) + g(a)$

Because $a \geq 0$, from $f(0) = 0$ and $f'(a) = -ae^{-a} \leq 0$, we conclude that $f(a) \leq 0$, so

$$N'(\mathbf{i}) = 2^{\mathbf{i}} (\ln 2) f(a) \leq 0$$

Let $h(a) = N(0) = (a + 2)e^{-a} + a - 2$, then $h(0) = 0$ and $h'(a) = -f(a) \geq 0$, we conclude that: $h(a) = N(0) \geq 0$.

From $N(0) \geq 0$ and $N'(\mathbf{i}) \leq 0$, we conclude that for all $\mathbf{i} \leq 0$, $N(\mathbf{i}) \geq N(0) \geq 0$.

Hence, $\forall \mathbf{i} \leq 0, 0 \leq \mathbf{r} < \Delta : \frac{\partial E}{\partial \mathbf{i}}(\mathbf{i}, \mathbf{r}) \geq 0$

□

Lemma 5.2 derives the error-bound of Interp-err of Φ^- in the range $(-\infty, -1]$. Note that for the range $(-1, 0)$, Φ^- is calculated by the co-transformation technique, the error-bound of which is derived in Section 7.

LEMMA 5.2. $\forall x \leq 0$:

$$|\Phi^-(x) - \hat{\Phi}_T^-(x)| \leq -E_{\Delta}^-(x)$$

PROOF. The proof is very similar to that of Lemma 5.1 See Appendix B for proof's details.

□

Theorem 5.3 derives the total error-bound of computing Φ^+ and Φ^- using first-order Taylor approximation.

THEOREM 5.3. *Let ϵ be the machine-epsilon of the fixed-point representation of the LNS under consideration. Let $E_M^+ = E_{\Delta}^+(0)$, and $E_M^- = -E_{\Delta}^-(x)$. Then*

$$|\Phi(x) - \tilde{\Phi}_T(x)| < E_M + (2 + \Delta)\epsilon$$

PROOF. Applying the absolute-value norm inequality $|\sum a_i| \leq \sum |a_i|$:

$$\begin{aligned} |\Phi(x) - \tilde{\Phi}_T(x)| &\leq |\Phi(x) - \hat{\Phi}_T(x)| + |\hat{\Phi}_T(x) - \tilde{\Phi}_T(x)| \\ &= E_M + |\hat{\Phi}_T(x) - \tilde{\Phi}_T(x)| \end{aligned}$$

From Equation 1 and Equation 6, $\hat{\Phi}_T(x) - \tilde{\Phi}_T(x)$ can be re-written as $a_1 + a_2 + a_3$, where

$$a_1 = \Phi(\mathbf{i}) - \bar{\Phi}(\mathbf{i})$$

$$a_2 = \mathbf{r}(\Phi'(\mathbf{i}) - \bar{\Phi}'(\mathbf{i}))$$

$$a_3 = \mathbf{r}\bar{\Phi}'(\mathbf{i}) - \text{rnd}(\mathbf{r}\bar{\Phi}'(\mathbf{i}))$$

⁵Since $\frac{\partial^2 E}{\partial \mathbf{r}^2}(\mathbf{i}, \mathbf{r})$ is strictly greater than 0, we conclude that if $\mathbf{r} > 0$ then $E(\mathbf{i}, \mathbf{r}) > 0$

⁶When $\mathbf{r} > 0$, we can replace all \geq and \leq in the rest of the proof by $>$ and $<$ correspondingly to prove that $\frac{\partial E}{\partial \mathbf{i}}(\mathbf{i}, \mathbf{r}) > 0$

Apply the absolute-value norm inequality $|\sum a_i| \leq \sum |a_i|$ again:

$$|\hat{\Phi}_T(x) - \tilde{\Phi}_T(x)| \leq |a_1| + |a_2| + |a_3|$$

From $|a_1|, |a_3|, |\Phi'(i) - \overline{\Phi'}(i)| \leq \epsilon$ (as they are errors of fixed-point rounding) and $0 \leq r < \Delta$:

$$|\hat{\Phi}_T(x) - \tilde{\Phi}_T(x)| < (2 + \Delta)\epsilon$$

Hence, the final error-bound of first-order Taylor approximation is obtained as:

$$|\Phi(x) - \tilde{\Phi}_T(x)| < E_M + (2 + \Delta)\epsilon$$

□

6 RIGOROUS ERROR BOUND OF THE ERROR CORRECTION TECHNIQUE

This section mentions in full detail the derivation of the rigorous error-bound of computing Φ^+ and Φ^- using the error-correction technique, together with the formal mathematical proof. The structure of this section is shown in Figure 6 and the intuition of the proof was briefly mentioned in Section 4.2. For a quick recall, there are four sources of error of interpolating by the error-correction technique: Ratio-err, Index-err, Tab-err and Mul-err. The error-bound of Ratio-err are derived in Lemma 6.3 (for Φ^+) and Lemma 6.6 (for Φ^-). The error-bound of Index-err are derived in Lemma 6.4 (for Φ^+) and Lemma 6.7 (for Φ^-). Finally, Theorem 6.8 accumulates the error-bounds of Ratio-err and Index-err with those of Tab-err and Mul-err to derives the total error-bound.

Recall that we defined $Q(i, r) = P(i - r) = P(x)$. Similar to the $E(i, r)$ in the proof of Lemma 5.1, for the sake of deriving the error-bound, it is safe to consider the domain of i to be $\mathbb{R}_{\leq 0}$. Lemma 6.1 derives the limit of $Q^+(i, r)$ and $Q^-(i, r)$ when $i \rightarrow -\infty$, which later will be proved to be the supremum of $Q^+(i, r)$ and infimum of $Q^-(i, r)$.

LEMMA 6.1.

$$\lim_{i \rightarrow -\infty} Q^+(i, r) = \lim_{i \rightarrow -\infty} Q^-(i, r) = \frac{2^{-r} + r \ln 2 - 1}{2^{-\Delta} + \Delta \ln 2 - 1}$$

PROOF. From the formula of $P(x)$:

$$Q^+(i, r) = P^+(i - r) = \frac{E^+_T(i - r)}{E^+_\Delta(i)} = \frac{\Phi^+(i - r) - \Phi^+(i) + r(\Phi^+)'(i)}{\Phi^+(i - \Delta) - \Phi^+(i) + \Delta(\Phi^+)'(i)}. \quad (8)$$

Because $(\Phi^+)'(i) = \frac{2^i}{2^{i+1}}$, we rewrite $Q^+(i, r)$ as:

$$Q^+(i, r) = \frac{2^i r \ln 2 - (2^i + 1) \ln(2^i + 1) + (2^i + 1) \ln(2^{i-r} + 1)}{2^i \Delta \ln 2 - (2^i + 1) \ln(2^i + 1) + (2^i + 1) \ln(2^{i-\Delta} + 1)}. \quad (9)$$

Define $f(a, r) = ar \ln 2 - (a + 1) \ln(a + 1) + (a + 1) \ln(a2^{-r} + 1)$. Then

$$Q^+(i, r) = Q^+_a(a, r) = \frac{f(2^i, r)}{f(2^i, \Delta)}.$$

We have $\lim_{a \rightarrow 0} f(a, r) = f(0, r) = 0$ and

$$\lim_{a \rightarrow 0} \frac{\partial f(a, r)}{\partial a} = \lim_{a \rightarrow 0} \left(r \ln 2 - \ln(a + 1) - 1 + \ln(a2^{-r} + 1) + \frac{2^{-r}(a + 1)}{a2^{-r} + 1} \right) = r \ln 2 - 1 + 2^{-r}.$$

Since $\lim_{i \rightarrow -\infty} 2^i = 0$ and $2^i > 0$ for all i , we can compute the limit of $Q^+(i, r)$ with L'Hopital's rule as follows

$$\lim_{i \rightarrow -\infty} Q^+(i, r) = \lim_{a \rightarrow 0^+} \frac{f(a, r)}{f(a, \Delta)} = \lim_{a \rightarrow 0^+} \frac{\frac{\partial}{\partial a} f(a, r)}{\frac{\partial}{\partial a} f(a, \Delta)} = \frac{2^{-r} + r \ln 2 - 1}{2^{-\Delta} + \Delta \ln 2 - 1}.$$

Similarly, we get the same result for $\lim_{i \rightarrow -\infty} Q^-(i, \mathbf{r})$ \square

Lemma 6.2 proves that $Q^+(i, \mathbf{r})$ is monotonically decreasing w.r.t i (its partial derivative over i is negative), when $i \leq 0$. The purpose of this Lemma is to show that the value of $Q^+(i, \mathbf{r})$ is inside the range $[Q_{min}^+(\mathbf{r}), Q_{sup}^+(\mathbf{r})]$ where $Q_{min}^+(\mathbf{r}) = Q^+(0, \mathbf{r})$ and $Q_{sup}^+(\mathbf{r}) = \lim_{i \rightarrow -\infty} Q^+(i, \mathbf{r})$. The range is shown in Figure 7; the small numerical value of the range verifies the observation that the error-ratio function (Figure 4) is roughly periodic.

LEMMA 6.2. $\forall i \leq 0, 0 \leq \mathbf{r} < \Delta$: $Q^+(i, \mathbf{r})$ is monotonically decreasing w.r.t i

PROOF. We prove the lemma by proving that $\forall i < 0, 0 < \mathbf{r} < \Delta$: $Q^+(i, \mathbf{r})$ is continuous and $\frac{\partial Q^+(i, \mathbf{r})}{\partial i} \leq 0$.

Similar to Lemma 5.1, we define $E(i, \mathbf{r}) = \Phi^+(i - \mathbf{r}) - (\Phi^+(i) - \mathbf{r}(\Phi^+)'(i))$.

From Equation 8, proving that $\forall i < 0, 0 < \mathbf{r} < \Delta$: $Q^+(i, \mathbf{r})$ is continuous is equivalent to proving that $\forall i < 0$: $E(i, \Delta) \neq 0$, which follows directly from footnote 5 as $\Delta > 0$.

For the rest of the proof, we prove that $\forall i < 0, 0 < \mathbf{r} < \Delta$: $\frac{\partial Q^+(i, \mathbf{r})}{\partial i} \leq 0$.

Let $h(i, \mathbf{r}) = E(i, \mathbf{r})(2^i + 1) \ln 2 = 2^i \mathbf{r} \ln 2 - (2^i + 1) \ln(2^i + 1) + (2^i + 1) \ln(2^{i-\mathbf{r}} + 1)$. Then from Equation 9:

$$\frac{\partial Q^+(i, \mathbf{r})}{\partial i} = \frac{\frac{\partial h}{\partial i}(i, \mathbf{r})h(i, \Delta) - \frac{\partial h}{\partial i}(i, \Delta)h(i, \mathbf{r})}{h(i, \Delta)^2}$$

Because

$$\frac{\partial Q^+(i, \mathbf{r})}{\partial i} \leq 0 \Leftrightarrow \frac{h(i, \mathbf{r})}{\frac{\partial h}{\partial i}(i, \mathbf{r})} \geq \frac{h(i, \Delta)}{\frac{\partial h}{\partial i}(i, \Delta)},$$

Let $g(i, \mathbf{r}) = \frac{h(i, \mathbf{r})}{\frac{\partial h}{\partial i}(i, \mathbf{r})}$. Since $\mathbf{r} < \Delta$, we prove $\forall i < 0, 0 < \mathbf{r} < \Delta$: $\frac{\partial Q^+(i, \mathbf{r})}{\partial i} \leq 0$ by proving that $\forall i < 0, 0 < \mathbf{r} < \Delta$: $g(i, \mathbf{r})$ is continuous ⁽¹⁾ and $\frac{\partial g}{\partial \mathbf{r}}(i, \mathbf{r}) \leq 0$ ⁽²⁾.

Proving ⁽¹⁾ is equivalent to proving that $\forall i < 0, 0 < \mathbf{r} < \Delta$: $\frac{\partial h}{\partial i}(i, \mathbf{r}) \neq 0$.

From $h(i, \mathbf{r}) = E(i, \mathbf{r})(2^i + 1) \ln 2$, we derive $\frac{\partial h}{\partial i}(i, \mathbf{r})$:

$$\frac{\partial h}{\partial i}(i, \mathbf{r}) = \left(\frac{\partial E}{\partial i}(i, \mathbf{r})(2^i + 1) + E(i, \mathbf{r})2^i \ln 2 \right) \ln 2$$

From the fact that if $\mathbf{r} > 0$ then $E(i, \mathbf{r}) > 0$ and $\frac{\partial E}{\partial i}(i, \mathbf{r}) > 0$ (see footnotes 5 and 6), we conclude that $\forall i < 0, 0 < \mathbf{r} < \Delta$: $\frac{\partial h}{\partial i}(i, \mathbf{r}) > 0$ and complete the proof for ⁽¹⁾.

To prove ⁽²⁾, we derive $\frac{\partial g}{\partial \mathbf{r}}(i, \mathbf{r})$: ⁷

$$\frac{\partial g}{\partial \mathbf{r}}(i, \mathbf{r}) = \frac{(B-1)K}{AM^2}$$

where

- $A = 2^i, B = 2^{\mathbf{r}}$
- $C = \ln(A + 1)$
- $D = \ln(A + B)$
- $M = AD - AC - BC + BD - B + 1$
- $K = A^2 \ln(A + B) - A^2 \ln(A + 1) - AB + A + B \ln B + B \ln(A + 1) - B \ln(A + B)$

Because $A > 0$ and $B \geq 1$ (since $i \leq 0, \mathbf{r} \geq 0$), $\frac{\partial g}{\partial \mathbf{r}}(i, \mathbf{r}) \leq 0$ is equivalent to $K \leq 0$ ⁽³⁾.

Considering K as a function of 2 variables A and B , we take the first and second derivatives of K w.r.t B :

$$\frac{\partial K}{\partial B}(A, B) = \frac{A^2 - B}{A + B} - A + \ln(A + 1) + \ln B - \ln(A + B) + 1$$

⁷The derivative is calculated using Sympy library

$$\frac{\partial^2 K}{\partial B^2}(A, B) = \frac{A^2(1-B)}{B(A+B)^2}$$

Substituting B for 1 in $\frac{\partial K}{\partial B}$, we get $\frac{\partial K}{\partial B}(A, 1) = 0$. Moreover, $\frac{\partial^2 K}{\partial B^2}(A, B) \leq 0$ since $A > 0$ and $B \geq 1$, we conclude that $\frac{\partial K}{\partial B}(A, B) \leq 0$. Similarly, substituting B for 1 in K , we get $K(A, 1) = 0$, together with $\frac{\partial K}{\partial B}(A, B) \leq 0$, we conclude that $K(A, B) \leq 0$ ⁽⁴⁾. The result of this lemma follows directly from ⁽²⁾, ⁽³⁾, and ⁽⁴⁾. \square

Lemma 6.3 derives the maximum of the range (i.e. $Q_{sup}^+(\mathbf{r}) - Q^+(0, \mathbf{r})$) w.r.t \mathbf{r} , which is the error-bound of the Ratio-err.

LEMMA 6.3. $\forall i \leq 0, c \leq 0, \mathbf{r} \in [0, \Delta)$:

$$|Q^+(i, \mathbf{r}) - Q^+(c, \mathbf{r})| < Q_{sup}^+(\mathbf{r}^*) - Q_{min}^+(\mathbf{r}^*)$$

where

$$\begin{aligned} Q_{sup}^+(\mathbf{r}) &= \lim_{i \rightarrow -\infty} Q^+(i, \mathbf{r}) = \frac{2^{-\mathbf{r}} + \mathbf{r} \ln 2 - 1}{2^{-\Delta} + \Delta \ln 2 - 1} \\ Q_{min}^+(\mathbf{r}) &= Q^+(0, \mathbf{r}) = \frac{\mathbf{r} \ln 2 + 2 \ln(1 + 2^{-\mathbf{r}}) - 2 \ln 2}{\Delta \ln 2 + 2 \ln(1 + 2^{-\Delta}) - 2 \ln 2} \\ \mathbf{r}^* &= \log_2 \frac{-X(2 \ln(X+1) - \ln X - 2 \ln 2)}{2X(\ln(X+1) - \ln X - \ln 2) + X - 1} \end{aligned}$$

where $X = 2^\Delta$

PROOF. From Lemma 6.1 and Lemma 6.2: $\forall i \leq 0, \mathbf{r} \in [0, \Delta) : Q^+(i, \mathbf{r}) \in [Q_{min}^+(\mathbf{r}), Q_{sup}^+(\mathbf{r})]$, then $\forall i \leq 0, c \leq 0, \mathbf{r} \in [0, \Delta) : |Q^+(i, \mathbf{r}) - Q^+(c, \mathbf{r})| < Q_{sup}^+(\mathbf{r}) - Q_{min}^+(\mathbf{r})$.

Let $F(\mathbf{r}) = Q_{sup}^+(\mathbf{r}) - Q_{min}^+(\mathbf{r})$, proving the lemma is equivalent to proving that $\mathbf{r}^* = \operatorname{argmax}_{[0, \Delta)} F$.

We take the first derivative of F ⁸:

$$F'(\mathbf{r}) = \frac{X2^{-\mathbf{r}}(2^{\mathbf{r}} - 1) \ln 2}{(2^{\mathbf{r}} + 1)(B - A)B} (A2^{\mathbf{r}} + B)$$

where

$$\begin{aligned} A &= 2X(\ln(X+1) - \ln X - \ln 2) + X - 1 \\ B &= X(2 \ln(X+1) - \ln X - 2 \ln 2) \end{aligned}$$

Note that $\mathbf{r}^* = \log_2(-B/A)$. Considering A and B as functions of X , since $X = 2^\Delta > 1$, performing basic function analysis, we can prove that $A < 0, B > 0$ and $B - A > 0$. Therefore, $F'(\mathbf{r}) = 0$ when $\mathbf{r} = \mathbf{r}^*$; $F'(\mathbf{r}) > 0$ when $0 < \mathbf{r} < \mathbf{r}^*$; and $F'(\mathbf{r}) < 0$ when $\mathbf{r} > \mathbf{r}^*$ (1). Because, $B - A > 0, \mathbf{r}^* = \log_2(-B/A) > 0$ (2). Since $F(0) = F(\Delta) = 0, \mathbf{r}^* < \Delta$; otherwise $F(0) < F(\Delta) = 0$, contradiction (3). Hence, from (1), (2), and (3), we conclude that $\mathbf{r}^* = \operatorname{argmax}_{[0, \Delta)} F$. \square

Lemma 6.4 derives error-bound of the Index-err.

LEMMA 6.4. Let Δ_P be the distance of two adjacent index values of P_c^+ tables and $\hat{\mathbf{r}}$ be the rounding of $\mathbf{r} \in [0, \Delta)$ in modulo Δ_P , i.e., $\hat{\mathbf{r}} = \left\lfloor \frac{x}{\Delta_P} \right\rfloor \Delta_P$, then

$$|Q^+(c, \mathbf{r}) - P_c^+(\hat{\mathbf{r}})| \leq 1 - Q_{min}^+(\Delta - \Delta_P)$$

PROOF. Let $E(i, \mathbf{r}) = \Phi(i - \mathbf{r}) - (\Phi(i) - \mathbf{r}\Phi'(i))$, then $\frac{\partial Q^+}{\partial \mathbf{r}}(c, \mathbf{r}) = \frac{1}{E(c, \Delta)} \frac{\partial E}{\partial \mathbf{r}}(c, \mathbf{r}) \geq 0$ (see proof of Lemma 5.1). Moreover because $\mathbf{r} > \hat{\mathbf{r}}$, we conclude that $Q^+(c, \mathbf{r}) - Q^+(c, \hat{\mathbf{r}}) \geq 0$. Therefore, $|Q^+(c, \mathbf{r}) - P_c^+(\hat{\mathbf{r}})| = Q^+(c, \mathbf{r}) - P_c^+(\hat{\mathbf{r}})$,

⁸The derivative is calculated using Sympy library

because $Q^+(c, \mathbf{r}) - P_c^+(\hat{\mathbf{r}}) = Q^+(c, \mathbf{r}) - Q^+(c, \hat{\mathbf{r}}) \geq 0$.

Let $t = \mathbf{r} - \hat{\mathbf{r}}$ and $F(\mathbf{r}, t) = Q^+(c, \mathbf{r}) - Q^+(c, \mathbf{r} - t)$, then

$$F(\mathbf{r}, t) = |Q^+(c, \mathbf{r}) - P_c^+(\hat{\mathbf{r}})| = \frac{E(c, \mathbf{r}) - E(c, \mathbf{r} - t)}{E(c, \Delta)}$$

Since $0 \leq \mathbf{r} < \Delta$ and $0 \leq t = \mathbf{r} - \hat{\mathbf{r}} < \Delta_P$:

$$F(\mathbf{r}, t) = |Q^+(c, \mathbf{r}) - P_c^+(\hat{\mathbf{r}})| < \max_{0 \leq t \leq \Delta_P, t \leq \mathbf{r} \leq \Delta} F(\mathbf{r}, t)$$

We will prove that $\max_{0 \leq t \leq \Delta_P, t \leq \mathbf{r} \leq \Delta} F(\mathbf{r}, t) = F(\Delta, \Delta_P)$, which is true if both partial derivatives of F are non-negative.

Taking the two partial derivatives of F :

$$\begin{aligned} \frac{\partial F}{\partial \mathbf{r}}(\mathbf{r}, t) &= \frac{1}{E(c, \Delta)} \left(\frac{\partial E}{\partial \mathbf{r}}(c, \mathbf{r}) - \frac{\partial E}{\partial \mathbf{r}}(c, \mathbf{r} - t) \right) \\ \frac{\partial F}{\partial t}(\mathbf{r}, t) &= \frac{\frac{\partial E}{\partial \mathbf{r}}(c, \mathbf{r} - t)}{E(c, \Delta)} \end{aligned}$$

In the proof for Theorem 1, we have proven that $\forall i \leq 0, 0 \leq \mathbf{r} < \Delta : E(\mathbf{i}, \mathbf{r}) \geq 0, \frac{\partial E}{\partial \mathbf{r}}(\mathbf{i}, \mathbf{r}) \geq 0$ and $\frac{\partial^2 E}{\partial \mathbf{r}^2}(\mathbf{i}, \mathbf{r}) \geq 0$.

From $E(\mathbf{i}, \mathbf{r}) \geq 0, \frac{\partial^2 E}{\partial \mathbf{r}^2}(\mathbf{i}, \mathbf{r}) \geq 0$ and $\mathbf{r} \geq \mathbf{r} - t$, we conclude that $\frac{\partial F}{\partial k}(k, t) \geq 0$.

From $E(\mathbf{i}, \mathbf{r}) \geq 0$ and $\frac{\partial E}{\partial \mathbf{r}}(\mathbf{i}, \mathbf{r}) \geq 0$, we conclude that $\frac{\partial F}{\partial t}(k, t) \geq 0$.

Hence,

$$|Q^+(c, \mathbf{r}) - P_c^+(\hat{\mathbf{r}})| < \max_{0 \leq t \leq \Delta_P, t \leq k \leq \Delta} F(k, t) = F(\Delta, \Delta_P) = 1 - P_c^+(\Delta - \Delta_P)$$

Finally, the lemma follows from the fact that $P_c^+(\Delta - \Delta_P) \geq Q_{min}^+(\Delta - \Delta_P)$ \square

Lemma 6.5, Lemma 6.6 and Lemma 6.7 are consecutively similar to Lemma 6.2, Lemma 6.3 and Lemma 6.4, but for Φ^- . The only difference is that $Q^-(\mathbf{i}, \mathbf{r})$ is increasing w.r.t \mathbf{i} in the range $(-\infty, -1]$ and the value of $Q^-(\mathbf{i}, \mathbf{r})$ is inside the range $(Q_{inf}^-(\mathbf{r}), Q_{max}^-(\mathbf{r})]$ where $Q_{inf}^-(\mathbf{r}) = \lim_{i \rightarrow -\infty} Q^+(\mathbf{i}, \mathbf{r})$ and $Q_{max}^-(\mathbf{r}) = Q^+(-1, \mathbf{r})$.

LEMMA 6.5. $\forall i \leq -1, 0 \leq \mathbf{r} < \Delta$:

$$\frac{\partial Q^-(\mathbf{i}, \mathbf{r})}{\partial i} \geq 0$$

PROOF. Similar to Lemma 6.2 \square

LEMMA 6.6. $\forall i \leq -1, c \leq -1, \mathbf{r} \in [0, \Delta)$:

$$|Q^-(\mathbf{i}, \mathbf{r}) - Q^-(c, \mathbf{r})| < Q_{max}^-(\mathbf{r}^*) - Q_{inf}^-(\mathbf{r}^*)$$

where

$$\begin{aligned} Q_{inf}^-(\mathbf{r}) &= \lim_{i \rightarrow -\infty} Q^-(\mathbf{i}, \mathbf{r}) = \frac{2^{-\mathbf{r}} + \mathbf{r} \ln 2 - 1}{2^{-\Delta} + \Delta \ln 2 - 1} \\ Q_{max}^-(\mathbf{r}) &= Q^-(-1, \mathbf{r}) = \frac{\ln(2 - 2^{-\mathbf{r}}) - \mathbf{r} \ln 2}{\ln(2 - 2^{-\Delta}) - \Delta \ln 2} \\ \mathbf{r}^* &= \log_2 \frac{2X \ln X - X \ln(2X - 1)}{2X \ln X - 2X \ln(2X - 1) + 2X - 2} \quad \text{with } X = 2^\Delta \end{aligned}$$

PROOF. The proof is similar to that of Lemma 6.3 but with some differences in function analysis. See Appendix C for proof details. \square

LEMMA 6.7. Let Δ_P be the distance of two adjacent index values of P_c^- tables and $\hat{\mathbf{r}}$ be the rounding of $\mathbf{r} \in [0, \Delta)$ in modulo Δ_P , i.e., $\hat{\mathbf{r}} = \left\lceil \frac{x}{\Delta_P} \right\rceil \Delta_P$, then

$$|Q^-(c, \mathbf{r}) - P_c^-(\hat{\mathbf{r}})| \leq 1 - Q_{inf}^-(\Delta - \Delta_P)$$

PROOF. Similar to Lemma 6.4 □

Theorem 6.8 derives the total error-bound of calculating Φ^+ and Φ^- using the error-correction technique by accumulating the error-bound derived in Lemma 6.3 and Lemma 6.4 for Φ^+ (similarly, Lemma 6.6 and Lemma 6.7 for Φ^-) with the fixed-point rounding errors.

THEOREM 6.8. Let ϵ be the machine-epsilon of the fixed-point representation of the LNS under consideration, and the error-bounds of Interp-err of first-order Taylor approximation: $E_M^+ = E_\Delta^+(0)$, $E_M^- = -E_\Delta^-(-1)$; the error-bounds of Ratio-err: $Q_R^+ = Q_{sup}^+(\mathbf{r}^*) - Q_{min}^+(\mathbf{r}^*)$, $Q_R^- = Q_{max}^-(\mathbf{r}^*) - Q_{inf}^-(\mathbf{r}^*)$; the error-bounds of Index-err: $Q_I^+ = 1 - Q_{min}^+(\Delta - \Delta_P)$, $Q_I^- = 1 - Q_{inf}^-(\Delta - \Delta_P)$, then

$$|\Phi(x) - \hat{\Phi}_{EC}(x)| \leq (4 + \Delta)\epsilon + E_M(Q_R + Q_I + \epsilon)$$

PROOF. Because $Q(\mathbf{i}, \mathbf{r}) = \frac{E_T(\mathbf{i}-\mathbf{r})}{E_\Delta(\mathbf{i})} = \frac{\Phi(x) - (\Phi(\mathbf{i}) - \mathbf{r}\Phi'(\mathbf{i}))}{E_\Delta(\mathbf{i})}$, we can write $\Phi(x)$ as: $\Phi(x) = \Phi(\mathbf{i}) - \mathbf{r}\Phi'(\mathbf{i}) + E_\Delta(\mathbf{i})Q(\mathbf{i}, \mathbf{r})$. Together with Equation 7, the error of computing $\Phi(x)$ using the error-correction technique is:

$$|\Phi(x) - \hat{\Phi}_{EC}(x)| = |\Phi(\mathbf{i}) - \bar{\Phi}(\mathbf{i}) + \text{rnd}(\mathbf{r}\bar{\Phi}'(\mathbf{i})) - \mathbf{r}\Phi'(\mathbf{i}) + E_\Delta(\mathbf{i})Q(\mathbf{i}, \mathbf{r}) - \text{rnd}(\bar{E}_\Delta(\mathbf{i})\bar{P}_c(\hat{\mathbf{r}}))|$$

We split $\Phi(\mathbf{i}) - \bar{\Phi}(\mathbf{i}) + \text{rnd}(\mathbf{r}\bar{\Phi}'(\mathbf{i})) - \mathbf{r}\Phi'(\mathbf{i}) + E_\Delta(\mathbf{i})Q(\mathbf{i}, \mathbf{r}) - \text{rnd}(\bar{E}_\Delta(\mathbf{i})\bar{P}_c(\hat{\mathbf{r}}))$ into the sum of 8 terms a_1, a_2, \dots, a_8 and derive the error-bound of the absolute value of each term as follows:

$$\begin{aligned} a_1 &= \Phi(\mathbf{i}) - \bar{\Phi}(\mathbf{i}) \Rightarrow |a_1| \leq \epsilon \\ a_2 &= \text{rnd}(\mathbf{r}\bar{\Phi}'(\mathbf{i})) - \mathbf{r}\bar{\Phi}'(\mathbf{i}) \Rightarrow |a_2| \leq \epsilon \\ a_3 &= \mathbf{r}\bar{\Phi}'(\mathbf{i}) - \mathbf{r}\Phi'(\mathbf{i}) \Rightarrow |a_3| \leq \mathbf{r}\epsilon \leq \Delta\epsilon \\ a_4 &= E_\Delta(\mathbf{i})Q(\mathbf{i}, \mathbf{r}) - E_\Delta(\mathbf{i})Q(c, \mathbf{r}) \Rightarrow |a_4| \leq E_M Q_R \\ a_5 &= E_\Delta(\mathbf{i})Q(c, \mathbf{r}) - E_\Delta(\mathbf{i})P_c(\hat{\mathbf{r}}) \Rightarrow |a_5| \leq E_M Q_I \\ a_6 &= E_\Delta(\mathbf{i})P_c(\hat{\mathbf{r}}) - E_\Delta(\mathbf{i})\bar{P}_c(\hat{\mathbf{r}}) \Rightarrow |a_6| \leq E_M \epsilon \\ a_7 &= E_\Delta(\mathbf{i})\bar{P}_c(\hat{\mathbf{r}}) - \bar{E}_\Delta(x)\bar{P}_c(\hat{\mathbf{r}}) \Rightarrow |a_7| \leq |\bar{P}_c(\hat{\mathbf{r}})|\epsilon \leq \epsilon \\ a_8 &= \bar{E}_\Delta(\mathbf{i})\bar{P}_c(\hat{\mathbf{r}}) - \text{rnd}(\bar{E}_\Delta(\mathbf{i})\bar{P}_c(\hat{\mathbf{r}})) \Rightarrow |a_8| \leq \epsilon \end{aligned}$$

Explanation: $|a_1|$, $|a_2|$, and $|a_8|$ are just errors of fixed-point rounding, so they are at most ϵ . The bounds of $|a_3|$, $|a_7|$ are obtained from the fixed-point rounding error-bound ϵ together with the facts that $\mathbf{r} < \Delta$ and $\bar{P}_c(\hat{\mathbf{r}}) \leq 1$. The bound of E_Δ is E_M , which is derived in Lemma 5.1 and Lemma 5.2. The bound of $|a_4|$ is obtained from the bound of the Ratio-err $|Q(\mathbf{i}, \mathbf{r}) - Q(c, \mathbf{r})|$, which is derived in Lemma 6.3 (for Φ^+) and Lemma 6.6 (for Φ^-). The bound of $|a_5|$ is obtained from the bound of the Index-err $|Q(c, \mathbf{r}) - P_c(\hat{\mathbf{r}})|$, which is derived in Lemma 6.4 (for Φ^+) and Lemma 6.7 (for Φ^-).

Finally, we apply the absolute-value norm inequality $|\sum a_i| \leq \sum |a_i|$ to derive the total error-bound:

$$|\Phi(x) - \hat{\Phi}_{EC}(x)| \leq (4 + \Delta)\epsilon + E_M(Q_R + Q_I + \epsilon)$$

□

Note that the error-bound derived in Theorem 6.8 does not depend on the constant c .

7 RIGOROUS ERROR BOUND OF THE CO-TRANSFORMATION TECHNIQUE

This section mentions in full detail the derivation of the error-bound of computing Φ^- in the range $(-1, 0)$ using the co-transformation technique, together with the formal mathematical proof. The overview of the derivation was mentioned in Section 4.3. For a quick recall, the co-transformation technique's computation involves computing $\Phi^-(x)$ by interpolation when x contains errors. In this case, the error-bound is derived by combining Lemma 7.1, which derives the error-bound of computing $\Phi^-(x)$ given the error-bound of x assuming that computing $\Phi^-(x)$ is error-free, with the error-bound of the interpolation technique, which is derived in Theorem 5.3 (for first-order Taylor approximation) or in Theorem 6.8 (for the error-correction technique). Finally, Theorem 7.2 perform step-by-step error-bound derivation for each of the three cases of the co-transformation technique's computation. The total error-bound is the maximum of three error-bounds.

LEMMA 7.1. For all $x, x^* \leq -1$ and $|x - x^*| \leq m$

$$|\Phi^-(x) - \Phi^-(x^*)| \leq \Phi^-(-1 - m) - \Phi^-(-1)$$

PROOF. Note that both the first and second derivatives of Φ^- are always negative:

$$\forall x : (\Phi^-)'(x) = \frac{-2^x}{1 - 2^x} < 0 \quad \text{and} \quad (\Phi^-)''(x) = \frac{-2^x \ln 2}{(1 - 2^x)^2} < 0$$

Without loss of generality, suppose that $x \geq x^*$, then $|\Phi^-(x) - \Phi^-(x^*)| = \Phi^-(x^*) - \Phi^-(x)$.

Let $t = x - x^*$ and $F(x, t) = \Phi^-(x - t) - \Phi^-(x)$, then $0 \leq t \leq m$ and

$$F(x, t) = |\Phi^-(x) - \Phi^-(x^*)| \leq \max_{0 \leq t \leq m, t \leq x \leq -1} F(x, t)$$

We will prove that $\max_{0 \leq t \leq m, t \leq x \leq -1} F(x, t) = F(-1, m)$, which is true if both partial derivatives of F are non-negative.

Since $x \geq x - t$ and $(\Phi^-)''(x) < 0$:

$$\frac{\partial F}{\partial x}(x, t) = (\Phi^-)'(x - t) - (\Phi^-)'(x) \geq 0$$

Since $(\Phi^-)'(x) < 0$:

$$\frac{\partial F}{\partial t}(x, t) = -(\Phi^-)'(x - t) \geq 0$$

Therefore, $\max_{0 \leq t \leq m, t \leq x \leq -1} F(x, t) = F(-1, m) = \Phi^-(-1 - m) - \Phi^-(-1)$.

Hence, $|\Phi^-(k) - \Phi^-(k^*)| \leq \Phi^-(-1 - m) - \Phi^-(-1)$ □

THEOREM 7.2. Let ϵ be the machine-epsilon of the fixed-point representation of the LNS under consideration and E_{Φ^-} be the error-bound of interpolating of Φ^- in the range $(-\infty, 1]$. The error-bound of computing $\Phi^-(x)$ when $x \in (-1, 0)$ using the co-transformation technique is:

$$\max(\epsilon + \Phi^-(-1 - 2\epsilon) - \Phi^-(-1) + E_{\Phi^-}, \quad \epsilon + \Phi^-(-1 - E_{k_2}) - \Phi^-(-1) + E_{\Phi^-})$$

where

$$E_{k_2} = 2\epsilon + \Phi^-(-1 - 2\epsilon) - \Phi^-(-1) + E_{\Phi^-}$$

PROOF. We derive the error-bound for each of the three cases of the co-transformation technique.

- **Case 1:** $x \in [-\Delta_a, 0)$: $\Phi^-(x)$ is indexed directly from T_a , so the error-bound is ϵ .

- **Case 2:** $x \in [-\Delta_b, -\Delta_a)$: r_b and r_a are error-free because their computations involve only operations that are error-free in fixed-point arithmetic, we consecutively derive the error-bound of computing k , $\Phi^-(k)$ and finally $\Phi^-(x)$. Let \tilde{k} and $\tilde{\Phi}^-$ be the results of the computations of k and Φ^- (with fixed-point rounding and interpolation errors). From the formula $k = x - \Phi^-(r_b) + \Phi^-(r_a)$, the error of computing k consists of the two fixed-point rounding errors of $\Phi^-(r_a)$ and $\Phi^-(r_b)$, so its error-bound is 2ϵ , (i.e. $|k - \tilde{k}| \leq 2\epsilon$). From the error-bound of computing k and Lemma 7.1, we get $|\Phi^-(k) - \tilde{\Phi}^-(\tilde{k})| \leq \Phi^-(-1 - 2\epsilon) - \Phi^-(-1)$. Next, because $\tilde{\Phi}^-(\tilde{k})$ is computed by interpolation, $|\Phi^-(\tilde{k}) - \tilde{\Phi}^-(\tilde{k})| \leq E_{\Phi^-}$, we apply the absolute-value norm inequality to derive the error-bound of computing $\Phi^-(k)$:

$$|\Phi^-(k) - \tilde{\Phi}^-(\tilde{k})| \leq |\Phi^-(k) - \Phi^-(\tilde{k})| + |\Phi^-(\tilde{k}) - \tilde{\Phi}^-(\tilde{k})| \leq \Phi^-(-1 - 2\epsilon) - \Phi^-(-1) + E_{\Phi^-}$$

Finally, from Equation 4, we accumulate the error-bound of computing $\Phi^-(k)$ with the fixed-point rounding error-bound of $\Phi^-(r_b)$, which is ϵ , to get the error-bound of computing $\Phi^-(x)$ in Case 2:

$$\epsilon + \Phi^-(-1 - 2\epsilon) - \Phi^-(-1) + E_{\Phi^-}$$

- **Case 3:** $x \in (-1, -\Delta_b)$: Similar to Case 2, all the terms r_c , r_{ab} , r_b and r_a are error-free, we consecutively derive the error-bound of computing k_1 , $\Phi^-(k_1)$, k_2 , $\Phi^-(k_2)$, and finally $\Phi^-(x)$. Let \tilde{k}_1 , \tilde{k}_2 and $\tilde{\Phi}^-$ be the actual results of computation of k_1 , k_2 and Φ^- . Because of the similarity in the formula of k_1 and that of k in Case 2, the error-bound of computing k_1 and $\Phi^-(k_1)$ is the same as that of computing k and $\Phi^-(k)$ in Case 2, which are 2ϵ and $\Phi^-(-1 - 2\epsilon) - \Phi^-(-1) + E_{\Phi^-}$. From the formula $k_2 = x + \Phi^-(r_b) + \Phi^-(k_1) - \Phi^-(r_c)$, we derive the error-bound of computing k_2 by accumulating the error-bound of computing $\Phi^-(k_1)$ with the fixed-point rounding error-bounds of $\Phi^-(r_b)$ and $\Phi^-(r_c)$ (both are ϵ). Let E_{k_2} be the error-bound of computing k_2 , then

$$E_{k_2} = 2\epsilon + \Phi^-(-1 - 2\epsilon) - \Phi^-(-1) + E_{\Phi^-}$$

Similar to how we derive the error-bound of computing $\Phi^-(k_1)$, the error-bound of computing $\Phi^-(k_2)$ is:

$$|\Phi^-(k_2) - \tilde{\Phi}^-(\tilde{k}_2)| \leq \Phi^-(-1 - E_{k_2}) - \Phi^-(-1) + E_{\Phi^-}$$

Finally, from Equation 5, we accumulate the error-bound of computing $\Phi^-(k_2)$ with the fixed-point rounding error-bound of $\Phi^-(r_c)$, which is ϵ , to get the error-bound of computing $\Phi^-(x)$ in Case 3:

$$\epsilon + \Phi^-(-1 - E_{k_2}) - \Phi^-(-1) + E_{\Phi^-}$$

Hence, the error-bound of computing $\Phi^-(x)$ when $-1 < x < 0$ with co-transformation technique is the maximum of the error-bounds of **Case 2** and **Case 3**, which is:

$$\max(\epsilon + \Phi^-(-1 - 2\epsilon) - \Phi^-(-1) + E_{\Phi^-}, \epsilon + \Phi^-(-1 - E_{k_2}) - \Phi^-(-1) + E_{\Phi^-})$$

where

$$E_{k_2} = 2\epsilon + \Phi^-(-1 - 2\epsilon) - \Phi^-(-1) + E_{\Phi^-}$$

□

8 NUMERICAL EXPERIMENTS

In this section, we perform two experiments. The first experiment (Section 8.1) use numerical testing to verify the correctness of the error-bounds' formulas of computing Φ^+/Φ^- using first-order Taylor approximation (derived in Theorems 5.3), the error-correction technique (derived in Theorems 6.8), and the co-transformation technique (derived in Theorems 7.2). For each technique, we test the error-bounds over different combination of values of the parameters: ϵ , Δ , Δ_P , Δ_a and Δ_b . For a quick recall, ϵ is the machine-epsilon of the fixed-point representation of the LNS under consideration; Δ are the separation of adjacent values in the look-up tables of Φ and Φ' ; Δ_P , Δ_a and Δ_b are those of tables P_c , T_a , and T_b . The second experiment (Section 8.2) uses the error-bounds' formulas to measure the impact of the interpolation techniques and the parameters on the magnitude of the relative error-bounds. The result of the experiment provides insight into the problem of selecting LNS designs that match some desired accuracy and hardware limitations.

8.1 Numerical verification of error-bound

The derived error-bound formulas contain non-polynomial functions Φ^+ and Φ^- , which cannot be handled by current automated theorem provers, and we chose an expedient way to check the bounds, namely through empirical testing. In the scope of our work, we perform the following experiment to verify the derived error-bound formulas with numerical values.

In total, we have derived the error-bound formulas for 6 cases of interpolation:

- (1) Computing $\Phi^+(x)$ for $x \in (-\infty, 0]$ using first-order Taylor approximation (Theorem 5.3).
- (2) Computing Φ^+ for $x \in (-\infty, 0]$ using the error-correction technique (Theorem 6.8).
- (3) Computing $\Phi^-(x)$ for $x \in (-\infty, -1]$ using first-order Taylor approximation (Theorem 5.3).
- (4) Computing Φ^- for $x \in (-\infty, -1]$ using the error-correction technique (Theorem 6.8).
- (5) Computing $\Phi^-(x)$ for $x \in (-1, 0)$ using the co-transformation technique combined with first-order Taylor approximation (Theorem 7.2 with E_{Φ^-} computed by Theorem 5.3).
- (6) Computing Φ^- for $x \in (-1, 0)$ using the co-transformation technique combined with error-correction technique (Theorem 7.2 with E_{Φ^-} computed by Theorem 6.8).

The computation of each case involves a set of parameters:

- Computing Φ^+/Φ^- using first-order Taylor involves ϵ and Δ
- Computing Φ^+/Φ^- using the error-correction technique involves ϵ , Δ and Δ_P
- Computing Φ^- using the co-transformation technique involves the parameters of the interpolation technique (first-order Taylor approximation or the error-correction technique) together with the two parameters: Δ_a and Δ_b .

Choice of Experimental Parameters. Note that although the computation of the error-correction technique involves the constant c , in our experiments, we do not consider c as a parameter for the following reasons:

- In actual LNS design, c is not selected arbitrarily, but rather carefully to minimize the error of computing Φ (see [8]). Finding the optimized value of c for each test case is beyond the scope of this experiment.
- For the purpose of verifying the validity of the error-bounds, if the error-bounds are valid on an *arbitrary* value of c , they are guaranteed to be valid on the value of c that minimizes the error of computing Φ . When evaluating a bound that uses error-correction techniques, we set $c = -4$, which is the optimized value of c in *European Logarithm Microprocessor*. [8].
- The error-bound of the error-correction technique *does not depend* on c .

We perform 76 test cases, which cover all 6 cases of interpolation with various combination of values of the parameters. The details of each test case are listed in Tables 4, 5, 6. For each test case, we pre-specify a sample set, an interpolation method, and the values of the parameters, then accordingly compute Φ^+/Φ^- for all values in the sample set. The error of computation is estimated by the difference between the computed results with the values of Φ^+/Φ^- computed directly in double-precision by Numpy library. The values of parameters are selected so that the size of all look-up tables are at most 2^{10} , which is suitable for them to be stored in ROM. During the experiment's design, we gradually increased the size and density of the sample sets such that they included enough points that represent extreme cases of the bounds' tightness.

Name	ϵ	Δ	Sample set
FT-Add1, FT-Sub1 FT-Add2, FT-Sub2 FT-Add3, FT-Sub3	2^{-8}	2^{-3} 2^{-4} 2^{-5}	For FT-Adds: $\{-k2^{-8} : k = 0, 1, \dots, 3 \times 2^8\}$ For FT-Subs: $\{-k2^{-8} - 1 : k = 0, 1, \dots, 3 \times 2^8\}$
FT-Add4, FT-Sub4 FT-Add5, FT-Sub5 FT-Add6, FT-Sub6	2^{-16}	2^{-4} 2^{-6} 2^{-8}	For FT-Adds: $\{-k2^{-16} : k = 0, 1, \dots, 3 \times 2^{16}\}$ For FT-Subs: $\{-k2^{-8} - 1 : k = 0, 1, \dots, 3 \times 2^{16}\}$
FT-Add7, FT-Sub7 FT-Add8, FT-Sub8 FT-Add9, FT-Sub9	2^{-32}	2^{-4} 2^{-6} 2^{-8}	For FT-Adds: $\{-k2^{-32} : k = 0, 1, \dots, 3 \times 2^{32}\}$ For FT-Subs: $\{-k2^{-8} - 1 : k = 0, 1, \dots, 3 \times 2^{32}\}$

Table 4. 18 test cases for computing Φ^+/Φ^- using first-order Taylor approximation.

Name	ϵ	Δ	Δ_P	Sample set
EC-Add1, EC-Sub1 EC-Add2, EC-Sub2 EC-Add3, EC-Sub3 EC-Add4, EC-Sub4 EC-Add5, EC-Sub5	2^{-8}	2^{-3}	2^{-6} 2^{-7}	For EC-Adds: $\{-k2^{-8} : k = 0, 1, \dots, 3 \times 2^8\}$ For EC-Subs: $\{-k2^{-8} - 1 : k = 0, 1, \dots, 3 \times 2^8\}$
2^{-4}		2^{-7} 2^{-8}		
2^{-5}		2^{-8}		
EC-Add6, EC-Sub6 EC-Add7, EC-Sub7 EC-Add8, EC-Sub8 EC-Add9, EC-Sub9 EC-Add10, EC-Sub10 EC-Add11, EC-Sub11	2^{-16}	2^{-4}	2^{-7} 2^{-8}	For EC-Adds: $\{-k2^{-16} : k = 0, 1, \dots, 3 \times 2^{16}\}$ For EC-Subs: $\{-k2^{-16} - 1 : k = 0, 1, \dots, 3 \times 2^{16}\}$
2^{-6}		2^{-9} 2^{-10}		
2^{-8}		2^{-11} 2^{-12}		
EC-Add12, EC-Sub12 EC-Add13, EC-Sub13 EC-Add14, EC-Sub14 EC-Add15, EC-Sub15 EC-Add16, EC-Sub16 EC-Add17, EC-Sub17	2^{-32}	2^{-4}	2^{-7} 2^{-8}	For EC-Adds: $\{-k2^{-16} : k = 0, 1, \dots, 3 \times 2^{16}\}$ For EC-Subs: $\{-k2^{-16} - 1 : k = 0, 1, \dots, 3 \times 2^{16}\}$
2^{-6}		2^{-9} 2^{-10}		
2^{-8}		2^{-11} 2^{-12}		

Table 5. 34 Test cases for computing Φ^+/Φ^- using error-correction technique.

Name	Interpolation	ϵ	(Δ_a, Δ_b)	Δ	Sample set		
Cotrans1	First-order Taylor	2^{-8}	$(2^{-6}, 2^{-3})$	2^{-3}	$\{-k2^{-8} : k = 0, 1, \dots, 2^8 - 1\}$		
Cotrans2				2^{-4}			
Cotrans3			$(2^{-5}, 2^{-2})$	2^{-3}			
Cotrans4				2^{-4}			
Cotrans5		2^{-16}	$(2^{-12}, 2^{-6})$	2^{-4}		$\{-k2^{-16} : k = 0, 1, \dots, 2^{16} - 1\}$	
Cotrans6				2^{-6}			
Cotrans7				$(2^{-10}, 2^{-5})$			2^{-4}
Cotrans8							2^{-6}
Cotrans9		2^{-32}	$(2^{-22}, 2^{-11})$	2^{-4}			
Cotrans10				2^{-6}			
Cotrans11				$(2^{-20}, 2^{-10})$	2^{-4}		
Cotrans12					2^{-6}		
Cotrans13	Error-correction	2^{-8}	$(2^{-6}, 2^{-3})$	2^{-3}	$\{-k2^{-8} : k = 0, 1, \dots, 2^8 - 1\}$		
Cotrans14				2^{-4}			
Cotrans15			$(2^{-5}, 2^{-2})$	2^{-3}			
Cotrans16				2^{-4}			
Cotrans17		2^{-16}	$(2^{-12}, 2^{-6})$	2^{-4}		$\{-k2^{-16} : k = 0, 1, \dots, 2^{16} - 1\}$	
Cotrans18				2^{-6}			
Cotrans19				$(2^{-10}, 2^{-5})$			2^{-4}
Cotrans20							2^{-6}
Cotrans21		2^{-32}	$(2^{-22}, 2^{-11})$	2^{-4}			
Cotrans22				2^{-6}			
Cotrans23				$(2^{-20}, 2^{-10})$	2^{-4}		
Cotrans24					2^{-6}		

Table 6. 24 test cases for computing Φ^- in the range $(-1, 0)$ using co-transformation technique. For the error-correction technique, we set $\Delta_P = 2^{-3}\Delta$.

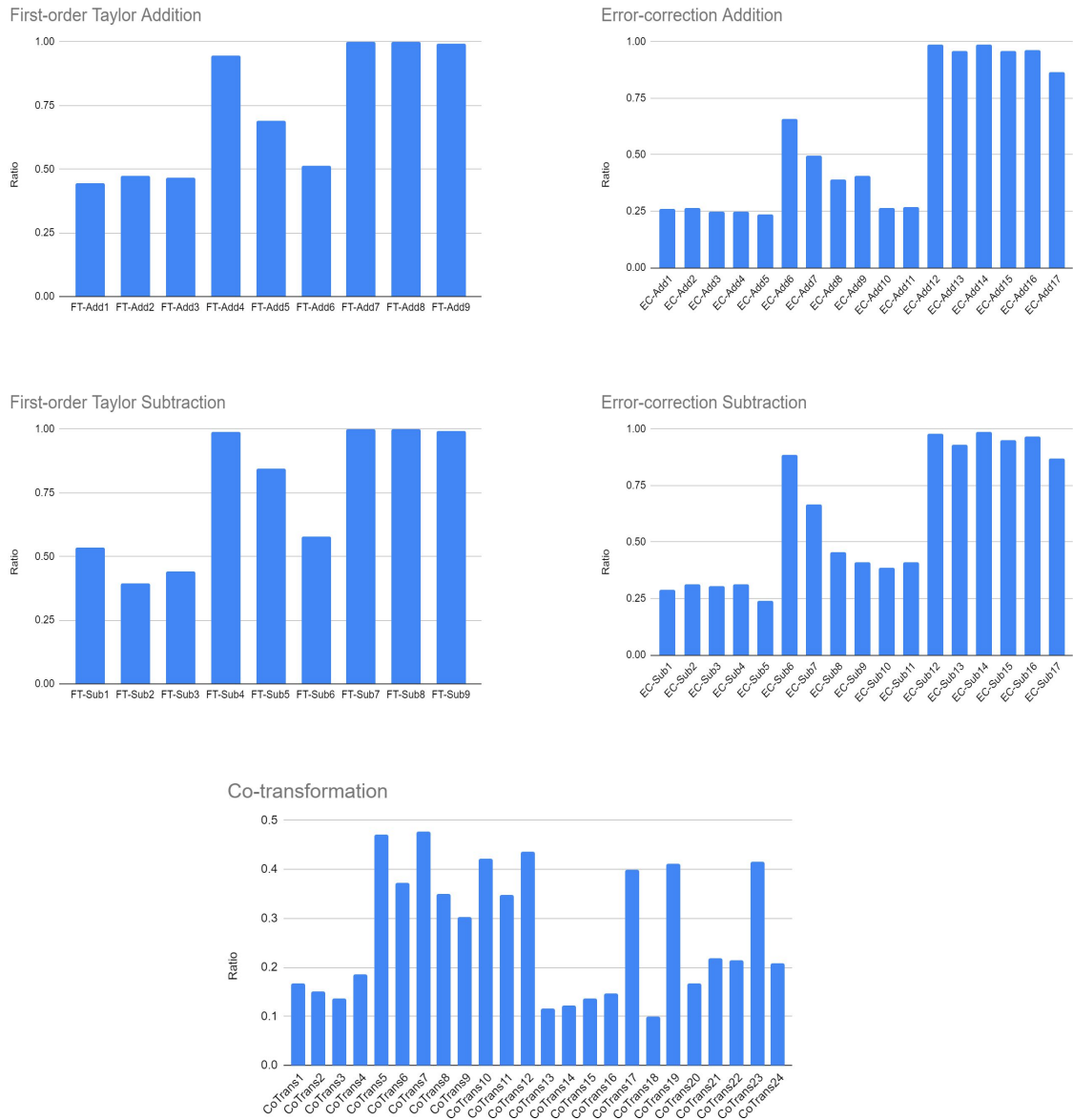


Fig. 9. The ratio of the maximum error of test cases to the error-bound computed by the derived formulas. Each column represents a test case in Tables 4, 5, 6.

Figure 9 shows the ratio of the maximum error of each test case to the derived error-bound. All the ratios are below 1.0, which strongly suggests that the error-bound is rigorous. Furthermore, the graph also indicates that the higher precision of the fix-point representation for implementing the LNS (the smaller ϵ), the tighter the error-bounds are. Figure 10 and 11 plot the histograms of the ratios of the errors of the testing samples to the error-bound of computing

addition and subtraction using first-order Taylor approximation and the error-correction technique with fixed values of $\Delta = 2^{-4}$, $\Delta_P = 2^{-7}$ and three values of $\epsilon : 2^{-8}, 2^{-16}$ and 2^{-32} . In other words, Figure 10 plots the histograms of test cases: FT-Add2, FT-Add4, FT-Add7, EC-Add3, EC-Add6, EC-Add12; and Figure 11 plots the histograms of test cases: FT-Sub2, FT-Sub4, FT-Sub7, EC-Sub3, EC-Sub6, EC-Sub12. Figure 12 plots similar histograms for the co-transformation technique combined with first-order Taylor approximation (test cases: Cotrans2, Cotrans5, Cotrans9) and the error-correction technique (test cases: Cotrans14, Cotrans17, Cotrans21). Those histograms indicate that although the maximum error is close to the error-bound in some cases, the ratios of most errors of testing samples to the error-bound are very small. In summary, our testing results establish the reliability of our error bounds —a valuable result that avoids over-provisioning in terms of hardware/software designs.

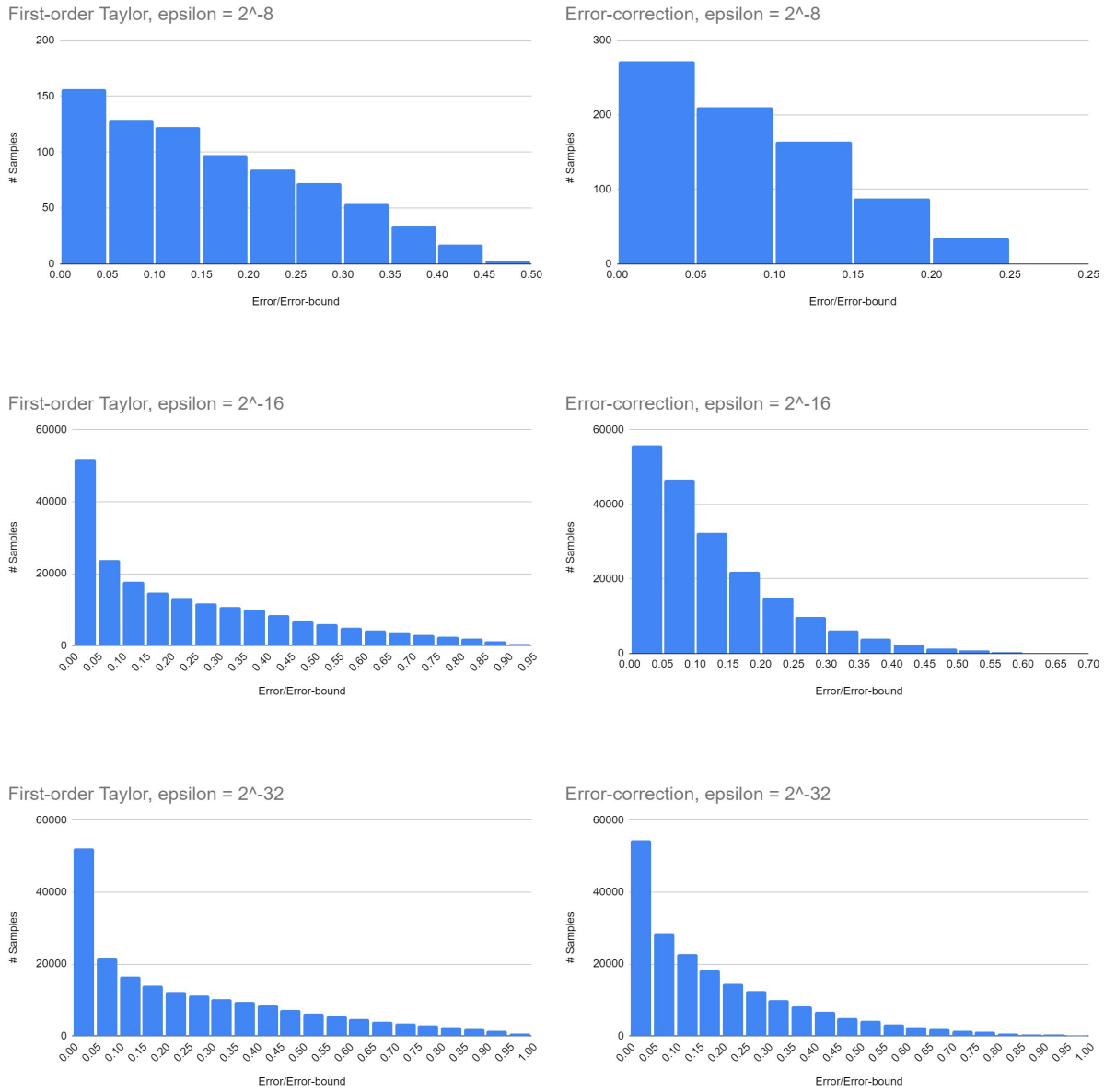


Fig. 10. The histograms of Error/Error-bound computing addition by first-order Taylor approximation and error-correction technique with different values of ϵ where Δ and Δ_P are fixed to be 2^{-4} and 2^{-7}

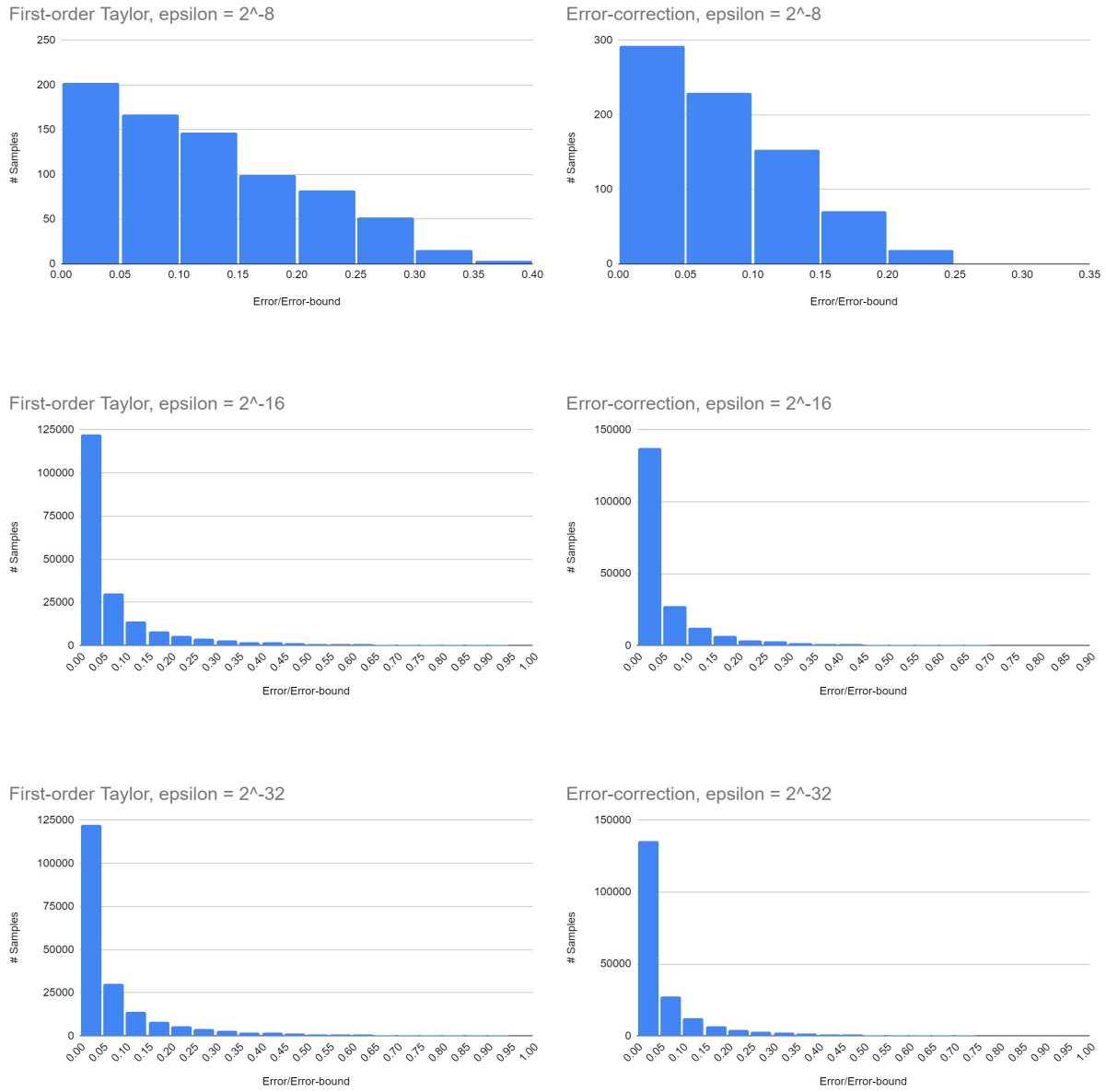


Fig. 11. The histograms of Error/Error-bound computing subtraction by first-order Taylor approximation and error-correction technique with different values of ϵ where Δ and Δ_P are fixed to be 2^{-4} and 2^{-7}

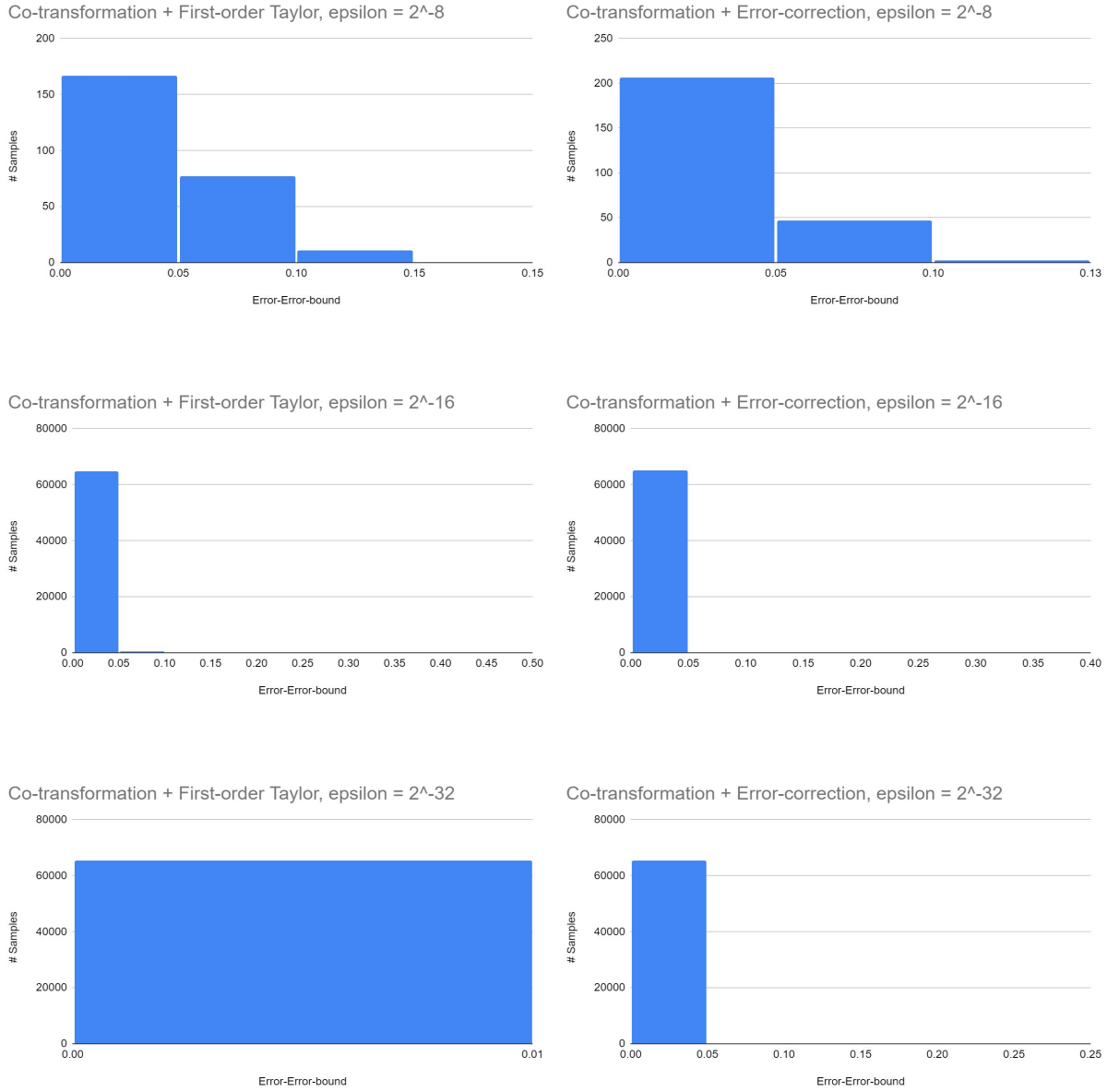


Fig. 12. The histograms of Error/Error-bound computing subtraction by co-transformation technique with different values of ϵ where Δ and Δ_P are fixed to be 2^{-4} and 2^{-7}

8.2 Magnitude of error-bound over parameters

One important application of deriving rigorous error-bound formulas is knowing how to tune the LNS parameters in order to achieve the desired error-bound for arithmetic operators. Note that although the computation of the co-transformation technique requires the two parameters Δ_a and Δ_b , our derived error-bound does not depend on those

parameters. In this section, we only consider the three parameters which effect the magnitude of the error-bounds: ϵ , Δ and Δ_P .

Table Sizes. Note that we can easily compute the sizes of look-up tables from ϵ , Δ , Δ_P and l , which is the number of bits used to represent the exponent of LNS:

- The size of the look-up tables for Φ , Φ' and E_Δ is $2^{l - \log_2 \Delta + \log_2 \epsilon}$
- The size of the look-up tables for P_c is Δ/Δ_P

The reader may find specific table sizes discussed in other LNS publications (such a discussion is outside the focus of this paper).

The following experiment provides insight into that problem by exploring the impact of the interpolation methods and their parameters on the magnitude of the error-bound. We perform this experiment on the bounds of the relative error (relative-error-bounds) of LNS's addition/subtraction instead of the error-bound of computing Φ^+/Φ^- , because the relative-error-bound is more widely used in high-dynamic-range, non-uniform-distributed number systems (such as LNS and floating-point) and can be easily computed from the error-bound of computing Φ^+/Φ^- by the following Corollary:

COROLLARY 8.1. *Let U be the the absolute error-bound of computing Φ^+/Φ^- , then the relative error-bound of LNS's addition/subtraction is 2^U*

PROOF. From the equations of LNS's addition/subtraction: $\log_2(2^i \pm 2^j) = i + \Phi^\pm(j - i)$, let err be the the absolute error of computing Φ^+/Φ^- . Because the fixed-point addition with i is error-free, err is also that of the absolute error of the fixed-point representation of the result of addition/subtraction ($\log_2(2^i \pm 2^j)$), and 2^{err} is the relative error of the real result. The Corollary's result follows from the additional fact that 2^x is a monotonical increasing function. \square

Specifically, the purpose of this experiment is to compare:

- The difference between the relative-error-bounds when applying first-order Taylor approximation versus the error-correction technique.
- The impact of Δ and Δ_P on the magnitude of the relative-error-bounds.
- The difference between the relative-error-bounds when we apply the co-transformation technique with first-order Taylor approximation and with the error-correction technique.

In this experiment, we compute the relative-error-bounds of addition and subtraction for 6 cases of Φ^+/Φ^- 's interpolation, which are mentioned at the beginning of Section 8.1. For each case, we compute the relative-error-bound for each value of Δ in the set: $\{2^{-3}, 2^{-4}, \dots, 2^{-10}, \}$. When the error-correction technique is applied, with each value of Δ , we compute the relative-error-bound for each value of Δ_P in the set $\{2^{-4}\Delta, 2^{-8}\Delta\}$. We choose $\epsilon = 2^{-24}$, which is the same as the machine epsilon of Floating-point 32. These constants were chosen in the European Logarithmic Microprocessor [13]. In MADAM, ϵ is much coarser, appearing to fall, according to [10], in the range $[2^{-10}, 2^{-8}]$, storing the numbers as integers but with a base of 2^{-10} with no error-correction employed.

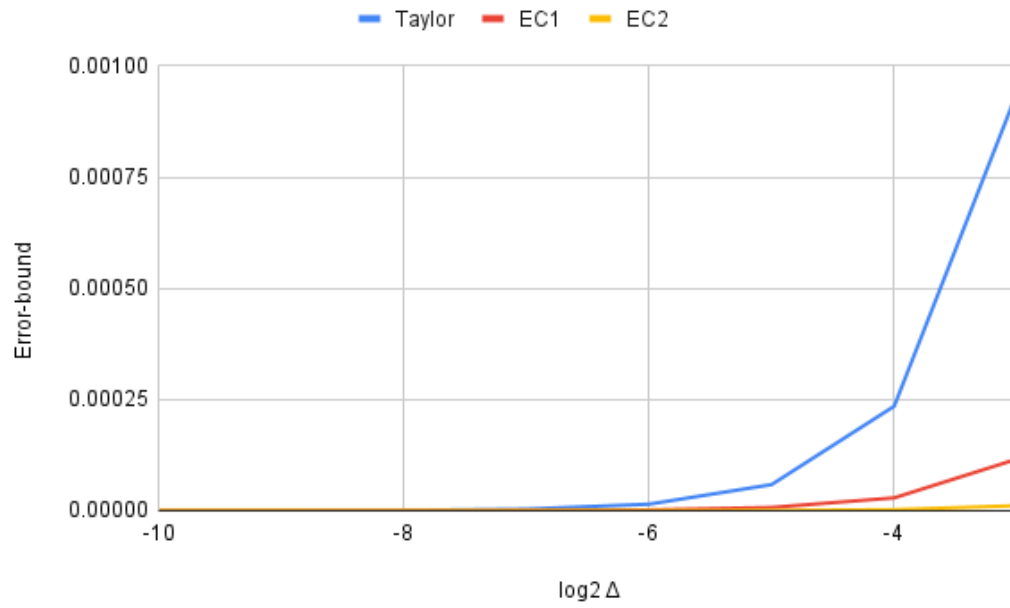


Fig. 13. Relative-error-bound of addition (of numbers falling within the whole domain supported by the underlying fixed-point representation) using first-order Taylor approximation (Taylor), error-correction with $\Delta_p = 2^{-4}\Delta$ (EC1) and with $\Delta_p = 2^{-8}\Delta$ (EC2)

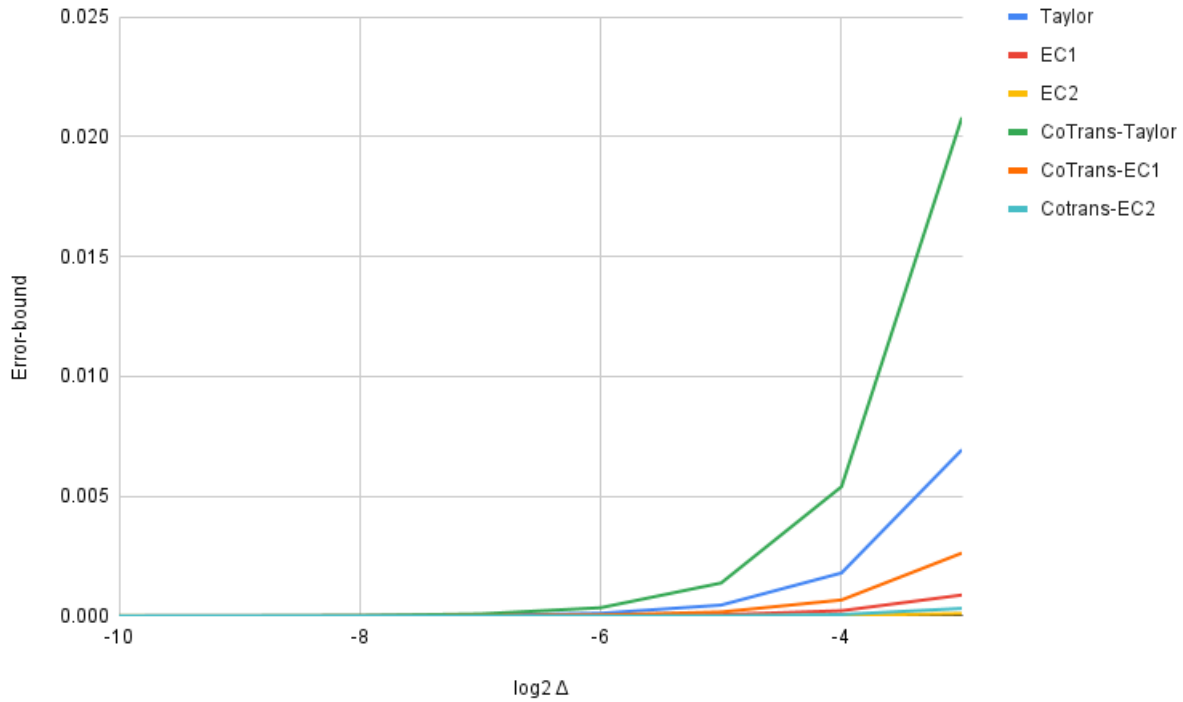


Fig. 14. Relative-error-bound of subtraction using first-order Taylor approximation (Taylor), error-correction with $\Delta_p = 2^{-4}\Delta$ (EC1) and with $\Delta_p = 2^{-8}\Delta$ (EC2) with and without co-transformation (Cotrans)

Figures 13 and 14 plot of the relative error-bounds of LNS's addition and subtraction over $\log_2 \Delta$. The key takeaways are the following:

- The greater the value of Δ is, the more significant the difference between the relative-error-bounds of using first-order Taylor approximation and those of using the error-correction technique, and the more significant difference between the relative-error-bounds of using an error-correction technique with different values of Δ_p (see Figure 13).
- The relative-error-bounds of using co-transformation technique show similar trends (see Figure 14).
- For the same interpolation technique (first-order Taylor approximation or error-correction) and the same values of parameters (Δ and Δ_p), the relative error-bounds of using co-transformation technique to compute Φ^- in $(-1, 0)$ is between 3 to 5 times greater than those of computing Φ^- outside of $(-1, 0)$ (i.e., without co-transformation) (see Figure 14).

However, there is an important observation that when $\Delta = 2^{-10}$, the relative error-bound of using first-order Taylor approximation is smaller than that of using the error-correction technique with both values of Δ_p (see Appendix). This observation can be explained according to the error-bound formulas of first-order Taylor approximation (Theorem 5.3) and of the error-correction technique (Theorem 6.8) as follows:

- With greater values of Δ , the error-bound of first-order Taylor approximation without fixed-point rounding (E_M) is significantly greater than ϵ , so, the error-bound of the error-correction technique is dominated by the term $E_M(Q_S + 1 - P_c(\Delta - \Delta_P) + \epsilon)$, while the error-bound of first-order Taylor approximation is dominated by the term E_M . Intuitively, both error-bounds are dominated by their interpolation error component, not their fixed-point rounding error component. Because Q_S and $1 - P_c(\Delta - \Delta_P)$ are error-bounds of Ratio-err and Index-err, the term $(Q_S + 1 - P_c(\Delta - \Delta_P) + \epsilon)$ is small. Therefore, the error-bound of the error-correction technique is much smaller than that of first-order Taylor approximation.
- In contrast, when Δ is small (approaches ϵ), the error-bound of the error-correction technique is dominated by the term $(4 + \Delta)\epsilon$, while the error-bound of first-order Taylor approximation is dominated by the term $(2 + \Delta)\epsilon$. Intuitively, in this case, both error-bounds are dominated by their fixed-point rounding error component; and because the error-correction technique requires more fixed-point calculations, its error-bound is greater than that of first-order Taylor approximation.

In summary, we can conclude that :

- Because the number of parameters is limited and the error-bounds computation is fast, our derived error-bound formulas can effectively support manual or brute-force parameter tuning for LNS's desired accuracy and ROM storage.
- In low-precision LNS, the error-correction technique may have a counter-effect to improving accuracy.

9 CONCLUDING REMARKS

We now briefly recap the contributions of this paper and also point out some future directions.

9.1 Contribution

We summarized our contribution as follows:

- (1) We derive rigorous error-bounds for LNS's addition and subtraction, which is based on combining ROM look-up tables with interpolation techniques. We cover the three main techniques, which are proposed in European Logarithm Microprocessor [13]: first-order Taylor approximation, the error-correction technique, and the co-transformation technique. The derived error-bound are parameterized by hardware implementation's parameters: $\epsilon, \Delta, \Delta_P, \Delta_a$ and Δ_b .
- (2) We verify the correctness and tightness of our error-bounds by empirical testing.
- (3) We perform experimental analysis about the impact of each parameter on the magnitude of the error-bound.

9.2 Future Directions

Adaptations to other LNS. For multi-based LNS designs such as [15] and [10], we can simply get the error-bound for base b by replacing \log_2 and $\ln 2$ in all of the error-bound formulas by \log_b and $\ln b$ respectively. For LNS designs which use different values of Δ for different segments in $(-\infty, 0)$ such as [13], similar to Theorem 5.3 the error-bound of first-ordered Taylor approximation of each segment $(a, b] \subset \mathbb{R}_{\leq 0}$ is $E_{\Delta_i}(b)$ with Δ_i is the value of Δ of the segment. The error-bound of the whole domain $\mathbb{R}_{\leq 0}$ is simply the maximum of all segments' error-bounds. Deriving rigorous error-bound for ROM-less LNS is beyond the scope of this paper. However, the formula of the error-bound of co-transformation technique is independent of the interpolation technique, so it is reusable to combine with any interpolation technique.

Mechanical Proof-Checking, Implementation Validation. Ideally, the rigorous error-bound analysis derived manually here must be formally analyzed through theorem-proving. Given the imminent uptake of LNS, we plan to invest in some efforts with respect to theorem-proving—at least assessing the tools that best suit our purposes. We also plan to prototype LNS on FPGAs or through efficient GPU kernel implementations, evaluating various tradeoffs and plugging them in lieu of other arithmetic schemes in machine learning and HPC (where appropriate). Given that table-less methods will be more hardware efficient, the analysis of popular schemes (e.g., Mitchell’s method) seem natural to pursue.

Pragmatic Considerations. The advantages of LNS with respect to multiplication and division will diminish with reduced bit sizes. This fact, together with the overheads of addition and subtraction error correction may make other number systems (or even traditional floating-point arithmetic) the best choice for very low number sizes. Where this cross-over occurs will be fruitful to research and discover. Last but not least, given the wide use of dot-products in both high-performance computing and machine learning, schemes to perform dot-products and obtain reasonable error bounds will also be of immense practical interest, and in our targeted list of goals.

REFERENCES

- [1] Shalf John. The future of computing beyond moore’s law, 2020. *Philosophical Transactions of the Royal Society*, <http://doi.org/10.1098/rsta.2019.0061>.
- [2] Daniel Reed, Dennis Gannon, and Jack Dongarra. Hpc forecast: Cloudy and uncertain. *Commun. ACM*, 66(2):82–90, jan 2023.
- [3] Haniel Barbosa, Clark Barrett, Martin Brain, Gereon Kremer, Hanna Lachnitt, Makai Mann, Abdalrhman Mohamed, Mudathir Mohamed, Aina Niemetz, Andres Nötzli, et al. cvc5: A versatile and industrial-strength smt solver. In *International Conference on Tools and Algorithms for the Construction and Analysis of Systems*, pages 415–442. Springer, 2022.
- [4] Leonardo De Moura and Nikolaj Bjørner. Z3: An efficient smt solver. In *International conference on Tools and Algorithms for the Construction and Analysis of Systems*, pages 337–340. Springer, 2008.
- [5] Bruno Dutertre. Yices 2.2. In *International Conference on Computer Aided Verification*, pages 737–744. Springer, 2014.
- [6] Jean-Michel Muller, Nicolas Brunie, Florent de Dinechin, Claude-Pierre Jeannerod, et al. *Handbook of Floating-Point Arithmetic*. Birkhauser, 2nd edition, 2018. Softcover reprint of the original edition.
- [7] Gaussian logarithm. Gaussian logarithm — Wikipedia, the free encyclopedia, 2021. [Online; 16 July 2023].
- [8] John N Coleman, El Chester, Christopher I Softley, and Jiri Kadlec. Arithmetic on the european logarithmic microprocessor. *IEEE Transactions on Computers*, 49(7):702–715, 2000.
- [9] Moisés Cywiak and David Cywiak. Sympy. In *Multi-Platform Graphics Programming With Kivy: Basic Analytical Programming for 2D, 3D, and Stereoscopic Design*, pages 173–190. Springer, 2021.
- [10] Jiawei Zhao, Steve Dai, Rangharajan Venkatesan, Brian Zimmer, Mustafa Ali, Ming-Yu Liu, Brucek Khailany, William J Dally, and Anima Anandkumar. Lns-madam: Low-precision training in logarithmic number system using multiplicative weight update. *IEEE Transactions on Computers*, 71(12):3179–3190, 2022.
- [11] Zhuo Liu, Yunan Yang, Zhenyu Pan, Anshujit Sharma, Amit Hasan, Caiwen Ding, Ang Li, Michael Huang, and Tong Geng. Ising-cf: A pathbreaking collaborative filtering method through efficient ising machine learning. In *Design Automation Conference*, 2023.
- [12] XLNS Research. <http://www.xlnsresearch.com/Default.htm>.
- [13] John N Coleman, Christopher I Softley, Jiri Kadlec, Rudolf Matousek, Milan Tichy, Zdenek Pohl, Antonin Hermanek, and Nico F Benschop. The european logarithmic microprocessor. *IEEE Transactions on Computers*, 57(4):532–546, 2008.
- [14] J Nicholas Coleman and R Che Ismail. Lns with co-transformation competes with floating-point. *IEEE Transactions on Computers*, 65(1):136–146, 2015.
- [15] Syed Asad Alam, James Garland, and David Gregg. Low-precision logarithmic number systems: beyond base-2. *ACM Transactions on Architecture and Code Optimization (TACO)*, 18(4):1–25, 2021.
- [16] J-M Muller, Alexandre Scherbyna, and Arnaud Tisserand. Semi-logarithmic number systems. *IEEE transactions on computers*, 47(2):145–151, 1998.
- [17] John N Mitchell. Computer multiplication and division using binary logarithms. *IRE Transactions on Electronic Computers*, (4):512–517, 1962.
- [18] Venkataraman Mahalingam and Nagarajan Ranganathan. Improving accuracy in mitchell’s logarithmic multiplication using operand decomposition. *IEEE Transactions on Computers*, 55(12):1523–1535, 2006.
- [19] Mark Arnold, Ed Chester, John Cowles, and Corey Johnson. Optimizing mitchell’s method for approximate logarithmic addition via base selection with application to back-propagation. In *2019 IEEE Nordic Circuits and Systems Conference (NORCAS): NORCHIP and International Symposium of System-on-Chip (SoC)*, pages 1–6. IEEE, 2019.

- [20] Mark Arnold, Ed Chester, and Corey Johnson. Training neural nets using only an approximate tableless lns alu. In *2020 IEEE 31st International Conference on Application-specific Systems, Architectures and Processors (ASAP)*, pages 69–72. IEEE, 2020.
- [21] Daisuke Miyashita, Edward H Lee, and Boris Murmann. Convolutional neural networks using logarithmic data representation. *arXiv preprint arXiv:1603.01025*, 2016.
- [22] Edward H Lee, Daisuke Miyashita, Elaina Chai, Boris Murmann, and S Simon Wong. Lognet: Energy-efficient neural networks using logarithmic computation. In *2017 IEEE International Conference on Acoustics, Speech and Signal Processing (ICASSP)*, pages 5900–5904. IEEE, 2017.
- [23] Matteo Croci, Massimiliano Fasi, Nicholas J Higham, Theo Mary, and Mantas Mikaitis. Stochastic rounding: implementation, error analysis and applications. *Royal Society Open Science*, 9(3):211631, 2022.
- [24] Normand Belanger and Yvon Savaria. On the design of a double precision logarithmic number system arithmetic unit. In *2006 IEEE North-East Workshop on Circuits and Systems*, pages 241–244. IEEE, 2006.
- [25] Mark G Arnold, Thomas A Bailey, John R Cowles, and Mark D Winkel. Arithmetic co-transformations in the real and complex logarithmic number systems. *IEEE Transactions on Computers*, 47(7):777–786, 1998.
- [26] MSSM Basir, RC Ismail, and SZM Naziri. An investigation of extended co-transformation using second-degree interpolation for logarithmic number system. In *2020 FORTEL-International Conference on Electrical Engineering (FORTEL-ICEE)*, pages 59–63. IEEE, 2020.
- [27] MSSM Basir, RC Ismail, and MNM Isa. A novel double co-transformation for a simple and memory efficient logarithmic number system. In *2020 IEEE International Conference on Semiconductor Electronics (ICSE)*, pages 25–28. IEEE, 2020.
- [28] Youri Popoff, Florian Scheidegger, Michael Schaffner, Michael Gautschi, Frank K Gürkaynak, and Luca Benini. High-efficiency logarithmic number unit design based on an improved cotransformation scheme. In *2016 Design, Automation & Test in Europe Conference & Exhibition (DATE)*, pages 1387–1392. IEEE, 2016.
- [29] RC Ismail, SAZ Murad, R Hussin, and JN Coleman. Improved subtraction function for logarithmic number system. *Procedia Engineering*, 53:387–392, 2013.
- [30] Venkataraman Mahalingam and Nagarajan Ranganathan. Improving accuracy in mitchell’s logarithmic multiplication using operand decomposition. *IEEE Transactions on Computers*, 55(12):1523–1535, 2006.
- [31] R Che Ismail and J Nicholas Coleman. Rom-less lns. In *2011 IEEE 20th Symposium on Computer Arithmetic*, pages 43–51. IEEE, 2011.
- [32] I Orginos, Vassilis Paliouras, and Thanos Stouraitis. A novel algorithm for multi-operand logarithmic number system addition and subtraction using polynomial approximation. In *Proceedings of ISCAS’95-International Symposium on Circuits and Systems*, volume 3, pages 1992–1995. IEEE, 1995.

APPENDIX

A Proof of the correctness of the co-transformation technique

PROOF. We prove the correctness of each case:

- **Case 1:** Trivial
- **Case 2:** From the definition of r_b and r_a :

$$2^i - 2^j = (2^i - 2^{j+r_a}) - (2^j - 2^{j+r_a}) = 2^{i+\Phi^-(r_b)} - 2^{j+\Phi^-(r_a)}$$

The subtraction $2^i - 2^j$ is transformed into the subtraction of $2^{i+\Phi^-(r_b)} - 2^{j+\Phi^-(r_a)}$.

We apply the LNS subtraction’s formula:

$$\log_2(2^{i+\Phi^-(r_b)} - 2^{j+\Phi^-(r_a)}) = i + \Phi^-(r_b) + \Phi^-(j + \Phi^-(r_a) - i - \Phi^-(r_b)) = i + \Phi^-(r_b) + \Phi^-(k)$$

It is obvious that r_a and r_b are among the index values of T_a and T_b , so $\Phi^-(r_a)$ and $\Phi^-(r_b)$ are indexed directly from T_a and T_b . Because $r_a \in [-\Delta_a, 0)$, $\Phi^-(r_a)$ is a great negative number, which ensures that $k < -1$ and $\Phi^-(k)$ can be computed by interpolation.

- **Case 3:**

From the definition of r_c, r_{ab}, r_b and r_a :

$$\begin{aligned} 2^i - 2^j &= (2^i - 2^{j+r_{ab}}) - ((2^j - 2^{j+r_b}) - (2^{j+r_{ab}} - 2^{j+r_b})) \\ &= 2^{i+\Phi^-(r_c)} - (2^{j+\Phi^-(r_b)} - 2^{j+r_{ab}+\Phi^-(r_a)}) \end{aligned}$$

We apply the LNS subtraction's formula:

$$\begin{aligned} 2^{j+\Phi^-(r_b)} - 2^{j+r_{ab}+\Phi^-(r_a)} &= 2^{j+\Phi^-(r_b)+\Phi^-(r_{ab}+\Phi^-(r_a)-\Phi^-(r_b))} = 2^{j+\Phi^-(r_b)+\Phi^-(k_1)} \\ &\Rightarrow 2^i - 2^j = 2^{i+\Phi^-(r_c)} - 2^{j+\Phi^-(r_b)+\Phi^-(k_1)} \end{aligned}$$

We apply the LNS subtraction's formula one more time:

$$\log_2(2^{i+\Phi^-(r_c)} - 2^{j+\Phi^-(r_b)+\Phi^-(k_1)}) = i + \Phi^-(r_c) + \Phi^-(j + \Phi^-(r_b) + \Phi^-(k_1) - i - \Phi^-(r_c)) = i + \Phi^-(r_c) + \Phi^-(k_2)$$

Similar to Case 2, $\Phi^-(r_a), \Phi^-(r_b), \Phi^-(r_c)$ are indexed directly from T_a, T_b , and T_c . Moreover, k_1 and k_2 are correspondingly dominated by the negative factor $\Phi^-(r_a)$ and $\Phi^-(r_b)$, which ensures that $k_1, k_2 < -1$, so $\Phi^-(k_1)$ and $\Phi^-(r_a)$ can be computed by interpolation. \square

B Proof of Lemma 5.2

PROOF. Let:

$$E(\mathbf{i}, \mathbf{r}) = \Phi^+_{-T}(x) - \Phi^-(x) = (\Phi^-(\mathbf{i}) - \mathbf{r}(\Phi^-)'(\mathbf{i})) - \Phi^-(\mathbf{i} - \mathbf{r})$$

Similar to the proof of Lemma 5.1, it is safe to consider the domain of \mathbf{i} to be $\mathbb{R}_{\leq -1}$ instead of $\Delta\mathbb{Z}_{\leq -1}$ when deriving error-bound. Then the lemma is proved by:

- (1) Proving that $\forall \mathbf{i} \leq -1, 0 \leq \mathbf{r} < \Delta : E(\mathbf{i}, \mathbf{r}) \geq 0$, so $E(\mathbf{i}, \mathbf{r}) = |E(\mathbf{i}, \mathbf{r})| = |\Phi^+(x) - \Phi^+_{-T}(x)|$
- (2) Proving that $\forall \mathbf{i} \leq -1, 0 \leq \mathbf{r} < \Delta : \frac{\partial E}{\partial \mathbf{r}}(\mathbf{i}, 0) \geq 0$ and $\frac{\partial E}{\partial \mathbf{i}}(\mathbf{i}, 0) \geq 0$, so $\max_{\mathbf{i} \in \mathbb{R}_{\leq 0}, 0 \leq \mathbf{r} < \Delta} E(\mathbf{i}, \mathbf{r}) < E(-1, \Delta) = -E^+_{\Delta}(-1)$

First, we take the first and second derivatives of $E(\mathbf{i}, \mathbf{r})$ w.r.t \mathbf{r} :

$$\frac{\partial E}{\partial \mathbf{r}}(\mathbf{i}, \mathbf{r}) = \frac{2^{\mathbf{i}}}{1 - 2^{\mathbf{i}}} - \frac{2^{\mathbf{i}-\mathbf{r}}}{1 - 2^{\mathbf{i}-\mathbf{r}}} \quad \text{and} \quad \frac{\partial^2 E}{\partial \mathbf{r}^2}(\mathbf{i}, \mathbf{r}) = \frac{2^{\mathbf{i}-\mathbf{r}} \ln 2}{(1 - 2^{\mathbf{i}-\mathbf{r}})^2}$$

From $\frac{\partial^2 E}{\partial \mathbf{r}^2}(\mathbf{i}, \mathbf{r}) > 0$ and $\frac{\partial E}{\partial \mathbf{r}}(\mathbf{i}, 0) = 0$, we conclude that $\forall \mathbf{i} \leq -1, 0 \leq \mathbf{r} < \Delta : \frac{\partial E}{\partial \mathbf{r}}(\mathbf{i}, \mathbf{r}) > 0$.

Then, because $E(\mathbf{i}, 0) = 0$, we conclude that $\forall \mathbf{i} \leq -1, 0 \leq \mathbf{r} < \Delta : E(\mathbf{i}, \mathbf{r}) \geq 0$.

We complete the proof by proving that $\forall \mathbf{i} \leq 0, 0 \leq \mathbf{r} < \Delta : \frac{\partial E}{\partial \mathbf{i}}(\mathbf{i}, \mathbf{r}) \geq 0$:

When $\mathbf{i} \leq -1, 0 \leq \mathbf{r} < \Delta$, let $a = \mathbf{r} \ln 2$

$$\frac{\partial E}{\partial \mathbf{i}}(\mathbf{i}, \mathbf{r}) = \frac{2^{\mathbf{i}}}{(1 - 2^{\mathbf{i}})^2 (1 - 2^{\mathbf{i}-\mathbf{r}})} (-2^{\mathbf{i}} f(a) + g(a))$$

$$\text{with } f(a) = ae^{-a} + e^{-a} - 1 \quad \text{and} \quad g(a) = e^{-a} + a - 1$$

Because $g(0) = 0$ and $g'(a) = 1 - e^{-a} \geq 0$ (for $a \geq 0$), we conclude that $g(a) \geq 0$. Moreover, $\mathbf{i} - \mathbf{r} \leq 0$ and $f(a) \leq 0$ for all $a \geq 0$ as proven in Lemma 5.1. Hence, $\forall \mathbf{i} \leq 0, 0 \leq \mathbf{r} < \Delta : \frac{\partial E}{\partial \mathbf{i}}(\mathbf{i}, \mathbf{r}) \geq 0$ \square

C Proof of Lemma 6.6

PROOF. From lemma 6.5: $\forall \mathbf{i} \leq -1, \mathbf{r} \in [0, \Delta) : Q^-(\mathbf{i}, \mathbf{r}) \geq Q^-(-1, \mathbf{r}) = Q^-_{max}(\mathbf{r})$ and $Q^-(\mathbf{i}, \mathbf{r}) > \lim_{\mathbf{i} \rightarrow -\infty} Q^-(\mathbf{i}, \mathbf{r}) = Q^-_{inf}(\mathbf{r})$ (See Lemma 6.1). Therefore, $\forall \mathbf{i} \leq 0, c \leq 0, r \in [0, \Delta) : |Q^-(\mathbf{i}, \mathbf{r}) - Q^-(c, \mathbf{r})| < Q^-_{max}(\mathbf{r}) - Q^-_{inf}(\mathbf{r})$.

Let $F(\mathbf{r}) = Q^-_{max}(\mathbf{r}) - Q^-_{inf}(\mathbf{r})$, we want to prove that $\mathbf{r}^* = \operatorname{argmax}_{[0, \Delta)} F$.

The first derivative of F has the form:

$$F'(\mathbf{r}) = \frac{-X \ln 2}{Y(2Y - 1)(X \ln X - X + 1)C} (AY^2 + BY + C)$$

where

$$Y = 2^r$$

$$A = 2X \ln X - 2X \ln(2X - 1) + 2X - 2$$

$$B = -4X \ln X + 3X \ln(2X - 1) - 2X + 2$$

$$C = 2X \ln X - X \ln(2X - 1)$$

There are at most two values of Y such that $F'(r) = 0$ (two solutions of $AY^2 + BY + C = 0$). The first value is $Y = 1$, so the second one is $Y = \frac{-B}{A} - 1 = 2^{r^*}$. Since $Y = 2^r$, there are two values of r such that $F'(r) = 0$: $r = 0$ and $r = r^*$. We observe that $F(0) = F(\Delta) = 0$ and according to lemma 6.5, $\forall i \leq -1, r \in [0, \Delta) : F(r) > 0$, so $\operatorname{argmax}_{[0, \Delta)} F \in (0, \Delta)$ since $F(r)$ is continuous. Moreover, $F'(\operatorname{argmax}_{[0, \Delta)} F) = 0$ since $F(r)$ is differentiable. Hence, $\operatorname{argmax}_{[0, \Delta)} F = r^*$. \square